GALVANOMAGNETIC PROPERTIES OF FERROMAGNETIC METALS AND ALLOYS

J. SMIT

GALVANOMAGNETIC PROPERTIES OF FERROMAGNETIC METALS AND ALLOYS

PROEFSCHRIFT

TER VERKRIJGING VAN DE GRAAD VAN
DOCTOR IN DE WIS- EN NATUURKUNDE
AAN DE RIJKSUNIVERSITEIT TE LEIDEN
OP GEZAG VAN DE RECTOR MAGNIFICUS
DR A. E. VAN ARKEL, HOOGLERAAR IN DE
FACULTEIT DER WIS- EN NATUURKUNDE,
PUBLIEK TE VERDEDIGEN OP WOENSDAG
11 APRIL 1956 TE 16 UUR

DOOR

JAN SMIT

NATUURKUNDIG INGENIEUR
GEBOREN TE MIDWOUD IN 1921

Promotor: Prof. Dr H. B. G. Casimir

STELLINGEN

I

De klassieke benaming „spin" voor de interne beweging van het electron is in sommige opzichten misleidend.

II

Het gebruik van een anisotrope relaxatietijd in de theorie der geleiding van metalen is, ook in de gebruikelijke benadering, niet algemeen genoeg. Beter is het in dat geval een anisotrope „vrije weglengte" in te voeren, welke niet evenwijdig aan de snelheid, behorende bij de beschouwde één-electron toestand, behoeft te zijn.

J. Smit, Physica **18**, 587 (1952).

III

In de theorie van de verandering van de electrische weerstand van metalen door een magnetisch veld, zoals die door Davis is gegeven, wordt ten onrechte geen rekening gehouden met het feit dat de verandering van de verdelingsfunctie der electronen tengevolge van het magnetische veld gevonden dient te worden als oplossing van een integraalvergelijking.

L. Davis, Phys. Rev. **56**, 93 (1939).

IV

Uit de experimentele resultaten voor de verandering van de thermo-electrische kracht door mechanische schuifspanningen voor de metalen koper, zilver en goud, geruggesteund door metingen van de verandering van de electrische weerstand, kan worden geconcludeerd dat bij deze metalen in de golfvectorruimte het Fermi-oppervlak raakt aan de grens van de eerste Brillouin-zone.

G. Borelius, Handb. der Metallphysik I, Leipzig (1935), p. 410.
M. J. Druyvesteyn, Physica **8**, 748 (1951).

V

Dat een star gelagerde, niet ingeklemde, roterende as met een aantal geconcentreerde massa's centrisch er op aangebracht, evenveel verschillende kritische toerentallen heeft, is ook gemakkelijk te begrijpen uit een beschouwing van de eigenschappen van de eigen- uitbuigingsvormen behorende bij deze toerentallen.

C. B. Biezeno, Proc. Kon. Ac. Wetensch. Amsterdam **43**, 1144 (1940).

VI

Bij de afleiding van de voorwaarden voor het optreden van ferromagnetische resonantie in niet-verzadigde specimina is het belangrijk de ontmagnetizerende werking voor de dynamische component van de magnetizatie, welke het gevolg is van de Weissgebieden-structuur, in aanmerking te nemen. In het bijzonder wordt de maximale grootte van het effectieve resonantieveld, veroorzaakt door ontmagnetizering, verhoogd van $2\pi M$, zoals dat geldt voor volledig gemagnetizeerde ellipsoiden, tot $4\pi M$.

D. Polder en J. Smit, Rev. mod. Phys. **25**, 89 (1953).
J. Smit en H. G. Beljers, Philips Res. Rep. **10**, 113 (1955).

VII

Als men de bij benadering geldende theoretische betrekking tussen de spectroscopische splitsingsfactor g, optredende bij ferromagnetische resonantie, en de magneto-mechanische factor g', welke bepalend is voor gyromagnetische effecten, niet uitdrukt door de vergelijking $g - 2 = 2 - g'$ maar door $\frac{1}{2} - \frac{1}{g} = \frac{1}{g'} - \frac{1}{2}$, dan geldt deze ook nog voor bijna gecompenseerde ferrimagnetica, waarin g zeer sterk van 2 kan afwijken.

C. Kittel, Phys. Rev. **76**, 743 (1949).
J. S. van Wieringen, Phys. Rev. **90**, 488 (1953).

VIII

De mechanische energie welke men bij constante temperatuur aan een systeem bestaande uit permanente magneten en weekijzer moet toevoeren om de configuratie reverzibel te veranderen, is gelijk aan de verandering van het gemiddelde van de vrije energie en de vrije enthalpie van de permanente magneten. Men zou deze grootheid de vrije enalpie kunnen noemen.

IX

De toeneming van de coercitieve kracht van Ticonal bij lage temperaturen wordt waarschijnlijk veroorzaakt door de kubische kristalanisotropie, welke laatste, althans bij een der soorten Ticonal, bij kamertemperatuur niet aanwezig is.

D. Lockhorst, A. van Itterbeek en G. J. van den Berg, Comm. 295a K. O. Lab., Appl. sci. Res. **B3**, 451 (1954).
E. A. Nesbitt en H. J. Williams, J. appl. Phys. **26**, 1217 (1955).

X

De wijze, waarop Snoek de grootte van de mechanische demping in α-ijzer, veroorzaakt door het springen van opgeloste koolstofatomen, in verband bracht met de roosterparameters van martensiet, impliceert dat de elastische constanten van gehard staal onafhankelijk zijn van het koolstofgehalte.

J. L. Snoek, Physica **8**, 711 (1941).

XI

Het thermodynamische vierkant, zoals dit door Koenig en Prins is ingevoerd, kan, door overgang op variabelen met de dimensie van energie, op logische wijze worden gefundeerd.

F. O. Koenig, J. chem. Phys. **3**, 29 (1935).
J. A. Prins, id. **16**, 65 (1948).

XII

Als men in een niet-relativistisch model een „oerknal" aanneemt, dan volgt hieruit o.m. dat de materiedichtheid van het uitdijende heelal „homogeen" moet zijn.

G. P. Ittmann, Ned. Tijdschrift voor Natuurkunde, **20**, 319 (1954).
Id. **21**, 277 (1955).

AAN MIJN OUDERS
AAN RIJKJE

CONTENTS

INLEIDING EN SAMENVATTING

Het blijkt experimenteel dat in een door een magnetisch veld verzadigd ferromagnetisch metaal of legering bij stroomdoorgang een extra electrisch veld optreedt in de richting van het tegelijkertijd aanwezige normale Hallveld. Dit verschijnsel zal worden aangeduid als het spontane Halleffect. De sterkte ervan kan het beste worden aangegeven met de grootte van de spontane Hallhoek, welke voor de in dit proefschrift onderzochte stoffen maximaal 0,02 rad is, of met de grootte van het magneetveld dat een even groot effect zou veroorzaken. Dit laatste is maximaal 450.000 oersted. Vooral dit effectieve magneetveld neemt sterk toe bij verhoging van de temperatuur, mits men de Curietemperatuur niet te dicht nadert.

Verder blijkt dat onder dezelfde omstandigheden de electrische weerstand anisotroop is, en wel is voor de in dit proefschrift onderzochte stoffen de weerstand in de richting van de magnetizatie maximaal 20% groter dan in een richting er loodrecht op. De sterkte van dit effect neemt af bij verhoging van de temperatuur.

Deze verschijnselen waren reeds bekend, maar nog niet verklaard. Door hun relatieve grootte krijgt men echter de indruk dat dit met de bestaande electronentheorie, tezamen met de kennis welke men heeft van het ferromagnetisme, toch mogelijk zou moeten zijn.

Om een meer volledig beeld van deze verschijnselen te verkrijgen, werd door schrijver dezes in de jaren 1949–1950 in het Kamerlingh Onnes Laboratorium de electrische weerstand van een aantal ferromagnetische metalen en legeringen in een magneetveld gemeten bij lage temperaturen en bij kamertemperatuur. In 1953 zijn in samenwerking met Dr J. Volger in het Philips Natuurkundig Laboratorium experimenten over het Halleffect aan een aantal van deze stoffen uitgevoerd in dit zelfde temperatuurgebied. De resultaten van deze onderzoekingen worden in dit proefschrift besproken, aangevuld met enkele meer theoretische beschouwingen.

In hoofdstuk I wordt, als grondslag voor latere beschouwingen, de bandenstructuur van nikkel behandeld, als zijnde karakteristiek voor die der midzijds kubische metalen en legeringen van de ijzergroep. Berekeningen van Fletcher worden overgedaan met een andere potentiaalfunctie, waarbij de correlatie tussen de posities van de electronen ter sprake komt terwijl tevens de 4*s*-electronen in de berekening worden betrokken, welke een groteinvloed op de bandenstructuur blijken te hebben.

In hoofdstuk II wordt het Halleffect besproken. Aangetoond wordt dat de toeneming van het spontane Halleffect bij verhoging van de temperatuur gecorreleerd is met die van de electrische weerstand. Bij een zuiver nikkelpreparaat verdwijnt bij lage temperatuur, tegelijk met de electrische weerstand, ook het spontane Halleffect. Bij ongeordende legeringen blijven beide eindig bij $T = 0$. In overeenstemming hiermee volgt uit het bewijs van H o u s t o n, volgens hetwelk een periodiek rooster geen weerstand heeft, dat ook het spontane Halleffect nul moet zijn, d.w.z. het magnetische veld dat werkt op de geleidingselectronen is dan gelijk aan de inductie B.

De verklaring van het effect moet dan ook worden gezocht in de invloed welke de spin-baanwisselwerking heeft op het verstrooiingsproces. Als resultaat vindt men dan dat het effectieve veld een fractie is van het spinbaanwisselwerkingsveld dat volgt uit de fijnstructuur van spectra ($\approx 10^7$ oersted).

Het is gebruikelijk het Halleffect te beschouwen als een eerste-, en de verandering van de electrische weerstand door een magnetisch veld als een tweede-orde-effect. Als men dit voor de spontane effecten ook doet, dan komt men tot de conlcusie dat het „tweede-orde-effect" (de relatieve anisotropie in de weerstand welke in hoofdstuk III wordt behandeld) ongeveer 10 keer zo groot is als het „eerste-orde-effect" (spontane Hallhoek) en niet enige tientallen malen kleiner, zoals men zou verwachten op grond van een nadere uitwerking van het mechanisme dat aansprakelijk is voor het spontane Halleffect. Dit mechanisme laat de component van het spinmoment in de richting van de macroscopische magnetizatie onveranderd, d.w.z. men gebruikt in de spin-baanwisselwerkingsoperator alleen de diagonaalelementen van de operator van het spinmoment. Dit is noodzakelijk om uitkomsten te verkrijgen welke lineair zijn in het magnetische moment, overeenkomende met de symmetrie van het Halleffect. Op grond van de experimentele resultaten moet dus voor de verklaring van de anisotropie van de weerstand wel teruggegrepen worden op de niet-diagonaalelementen van de operator van het spinmoment. De uitkomsten welke hiermee worden verkregen bevatten alleen even machten van het magnetisch moment. Men behoeft dus niet bang te zijn in de uitkomst van de theorie geconfronteerd te worden met een spontane Hallhoek van de orde van grootte $(0{,}2)^{\frac{1}{2}}$.

Om de weerstand-temperatuurkromme van nikkel te verklaren, nam M o t t aan dat door de roostertrillingen electronen veelvuldig van s- naar d-toestanden overgaan en omgekeerd, onder behoud van de richting van hun spinmoment. Bij lage temperaturen kunnen s-electronen met een spin parallel aan de resulterende magnetizatie deze overgangen niet maken, omdat de corresponderende d-toestanden alle bezet zijn, zodat deze s-electronen de minste weerstand ondervinden en het grootste gedeelte van de stroom voeren. Deze toestand verandert enigermate door de invoering van de spinbaanwisselwerking en in hoofdstuk III zal worden aangetoond dat de op-

tredende extra overgangen de anisotropie in de weerstand geven. Het blijkt experimenteel dat vreemde ferromagnetische ionen een grotere anisotropie geven dan roostertrillingen en niet-magnetische ionen. Dit volgt ook uit algemene theoretische beschouwingen. De grootte van het effect wordt geschat op ongeveer 5%, dat dus iets aan de kleine kant is.

Bij lage temperaturen treedt in de zuivere metalen ijzer en nikkel de normale toeneming van de weerstand in een magnetisch veld op. Voor ijzer kwam met zekerheid vast te staan dat het effectieve veld, dat op de geleidingselectronen werkt, B is, wat een bevestiging inhoudt van de in hoofd-II gedane uitspraken.

Het is mij een genoegen mijn erkentelijkheid te betuigen aan de Directie van het Natuurkundig Laboratorium der N.V. Philips' Gloeilampenfabrieken, die mij mede in staat stelde dit werk uit te voeren en de resultaten ervan te publiceren.

Dat ik gedurende een gedeelte van het onderzoek in persoonlijk contact heb mogen profiteren van de kennis en het inzicht van Dr J. L. Snoek†, beschouw ik als een groot voorrecht.

De Heren E. J. Haes, A. Schaafsma en J. van Weesel dank ik voor de verleende hulp bij de experimenten.

De Stichting Physica dank ik voor het gebruik van enig zetsel en enkele cliché's.

SUMMARY

In chapter I the band structure of the incomplete shell electrons in nickel has been calculated with the aid of a potential function different to that used by Fletcher. The correlation has been taken into account. The consideration of the *s* electrons substantially changes the band picture.

In chapter II experimental results concerning the Hall effect in ferromagnetic metals and alloys are given, together with a theoretical discussion on the origin of the spontaneous part. It is shown that the latter is correlated with the electrical resistivity, and in agreement with this view it vanishes for a pure nickel sample at low temperatures, *i.e.* the effective field is equal to B. This is merely a consequence of Houstons proof that a periodic lattice has no resistivity. For disordered alloys both effects remain finite near $T = 0$.

The theoretical explanation is based upon the anisotropic scattering due to spin-orbit interaction. In effect the moving electrons are electrically polarized due to this interaction. Though the order of magnitude of the effects can be accounted for, the models used are too simple to yield a satisfactory description.

For the explanation of the spontaneous Hall effect only the diagonal elements of the spin moment operator were used. However, for the calculation of the anisotropy in the resistivity of ferromagnetic metals and alloys it is necessary to employ the off-diagonal elements. Experiments and theory of this effect are described in chapter III. The theory given is an extension of the theory of Mott concerning the resistivity-temperature curve of nickel.

Superimposed on these purely ferromagnetic effects there is, of course, the normal increase in resistivity in a magnetic field. It is shown that for pure iron the effective field at low temperatures is equal to B, just as was found in the studies of the Hall effect for nickel.

CHAPTER I

THE BAND STRUCTURE OF THE INCOMPLETE SHELL ELECTRONS IN NICKEL

1. Introduction

Before discussing the galvanomagnetic properties of ferromagnetic metals it will prove necessary to first treat the electronic structure of these materials.

For the non-transition metals the electrical properties are determined by the *s* or *p* electrons of the outer shell only. The transition metals, however, also contain partially filled *d* shells. In the metals iron, cobalt and nickel these 3*d* electrons have uncompensated spins and at ordinary temperatures give rise to ferromagnetism, because of the exchange interactions between these electrons on neighbouring atoms. It is usually assumed that there are also electrons in the 4*s* and 4*p* states. These electrons presumably do not contribute to the net magnetic moment of the solid; they carry the greater part of the current.

The multi-electron wave function in solids is usually approximated by a product, or more generally a determinant, of one-electron wave functions. Because of the approximate nature there is a certain freedom in the choice of the latter functions. Usually two types of wave functions are used, *i.e.* the atomic type (H e i t l e r-L o n d o n) and the periodic type (B l o c h). Physically it means that we assume as a first approximation that the electrons are independent of each other, each moving in a fixed potential field caused by the nuclei and the other electrons. In the first scheme the electrons are assumed to stay around the ion at which they were in the isolated atom. In the second picture the electron is assumed to wander through the whole crystal, having equal probabilities of occurrence at equivalent sites in the crystal. If the atoms are far from each other, the first model gives a more realistic description, whereas for small distances the use of the latter is more justified. If we assume one electron per atom in the unfilled shell, then in the atomic model conductivity can only occur by the excitation of one of these electrons to a higher state in a neighbouring atom. In general this will require a large amount of energy, so we can say that metallic conductivity cannot occur. In this model these electrons will not contribute to

the specific heat at low temperatures. In the Bloch model the electrons move through the crystal, and their energies, being mainly kinetic, have a nearly continuous spectrum. An electric field can then produce transitions between states adjacent in the energy scale, *i.e.* the solid conducts electricity. These states will also give rise to a contribution proportional to T in the specific heat.

The latter model is therefore ideally suited for the treatment of the conduction electrons in metals and most essential features of metals are quite well understood with the aid of a theoretical description in terms of these wave functions.

For the *d* electrons in the transition metals the situation is more difficult. These orbits are smaller than those of the *s* electrons of the next shell, and therefore the overlapping of the wave functions of adjacent ions is less, and so also is the probability of an electron jumping over. The Heitler-London model seems, therefore, more adequate for these electrons, but then we encounter great difficulties. In nickel, for instance, the magnetic moment corresponds to the spin moment of 0.6 electrons per atom, so that one assumes that about 0.6 electrons are missing in the 3*d* shell. This non-integral number is not consistent with the Heitler-London model, since one cannot assume that 60% of the atoms have a hole in the *d* shell, and the remaining have none. Undoubtedly these holes have to move, so that over a time average all ions are identical. According to the Bloch model the electrons move independently so that the number of electrons at a certain moment in one ion is governed by the laws of probability. The electrons are subject to the Pauli principle, so that no more than two electrons (with opposite spin) can be in the same orbit. It has been shown by Van Vleck [1]) that in nickel for example, the highly ionized states having only 7 or 8 *d* electrons, have far too large a weight in the total Bloch wave function. As the formation of such states actually requires a large amount of energy, they will not occur very frequently in reality. Van Vleck therefore proposes the use of a wave function for nickel in which only d^9 and d^{10} states occur, but in which the electrons still may jump from one atom to an adjacent one (itinerant Heitler-London model). The movement of the electrons is therefore to some extent correlated. Unfortunately such a model cannot be handled mathematically. The high electronic specific heat at low temperatures (proportional to the absolute temperature T) in the transition metals reveals that a continuum of energy levels above the ground state exists. One is forced therefore to use an itinerant electron model for these 3*d* electrons.

The Bloch model is extensively used for the calculation of the properties of these 3*d* electrons and we shall in this chapter discuss a calculation of the energy bands in nickel given by Fletcher [2]) [3]). A different potential field will be used and the calculation will be extended by taking into account the 4*s* electrons.

The fact that in this approximation highly ionized states occur, is not as serious as one might think in the energy calculation. This is due to the fact that we assume, as we shall see in the next section, that the electrons move in a fixed potential field, which in any atomic polyhedron is almost identical to that occurring in the free atom, so that the high energy of these highly ionized states, which increases very strongly with the degree of ionization, does not enter into the calculation. Though in any perturbation theory the energy is always more accurate than the wave function used, in this case it is enhanced by the choice of the energy operator. This criticism of the band picture is therefore applicable to the wave function but to a far lesser extent to the energy calculated for it.

For the calculation of the band structure in the Bloch scheme we shall use the tight-binding approximation. It is agreed that near one ion the wave function has to resemble very much that of the free atom. The Bloch function is therefore built up from the atomic wave functions of all the ions of the lattice.

2. The tight-binding approximation

If there exist atomic one-electron wave functions for an atom centred around $\mathbf{r}_n$, which are denoted by $\varphi_j(\mathbf{r} - \mathbf{r}_n)$, then we can construct from it Bloch wave functions for a periodic crystal according to

$$\psi(\mathbf{k}, \mathbf{r}) = \Sigma_j \Sigma_n a_j(\mathbf{k})\, e^{i\mathbf{k}\mathbf{r}_n} \varphi_j(\mathbf{r} - \mathbf{r}_n), \tag{1}$$

where n is summed over all N lattice points and j over all possible atomic wave functions. In the tight-binding approximation it is assumed that one obtains the right wave functions for one band by taking in (1) only the atomic wave functions of one or a few shells. This will be the case if the atomic wave functions under consideration of neighbouring atoms do not overlap too much. In this section we shall only consider the $3d$ functions.

To the Hamilton operator $H_n^{(0)}(\mathbf{r})$ for an electron centred at $\mathbf{r}_n$ in the free atom an operator $H_n^{(1)}(\mathbf{r})$ is added so that

$$H(\mathbf{r}) = H_n^{(0)}(\mathbf{r}) + H_n^{(1)}(\mathbf{r})$$

is periodic. The Schroedinger equation gives then, after multiplication by an atomic wave function centred at the origin and integration:

$$\Sigma_j a_j(\mathbf{k}) \Sigma_n e^{i\mathbf{k}\mathbf{r}_n} \int \varphi_i^*(\mathbf{r})\, H\, \varphi_j(\mathbf{r} - \mathbf{r}_n)\, \mathrm{d}\tau = E(\mathbf{k})\, a_i(\mathbf{k}), \tag{2}$$

where it is assumed that

$$\int \varphi_i^*(\mathbf{r} - \mathbf{r}_n)\, \varphi_j(\mathbf{r} - \mathbf{r}_m)\, \mathrm{d}\tau = \delta_{ij}\, \delta_{nm}. \tag{3}$$

This assumption will in general not be satisfied by the atomic wave functions. It is always possible, however, to construct by linear combination of them a new set of "atomic" functions for which (3) is valid. It appears [4]) that by

using in (2) the true atomic wave functions, thus neglecting their lack of orthogonality, the relative error in the final **k**-dependent part of the energy is of the order of the overlap-integral times the number of nearest neighbours, which, according to Fletcher [3]), for the 3*d* functions of nickel is at the most 0.1, so this gives an error of the order of 10%. Furthermore we shall retain with Fletcher in (2) only the contributions of pairs of nearest neighbours. Estimation shows that this error is at most 10%.

Equation (2) represents a set (for the 3*d* electrons five) of homogeneous linear equations in the coefficients $a_i(\mathbf{k})$ which give rise to a determinantal equation with matrix elements

$$H_{ij} = E_i^{(0)}\,\delta_{ij} + \Sigma_n\, e^{i\mathbf{k}\mathbf{r}_n} \int \varphi_i^*(\mathbf{r})\, H_0^{(1)} \varphi_j(\mathbf{r} - \mathbf{r}_n)\, \mathrm{d}\tau, \tag{4}$$

where $E_j^{(0)}$ is the energy of the electron in the free atom wave function φ_j. It is the same for all the five 3*d* orbits. The summation over n in (4) refers only to nearest neighbours. For each value of **k** we then find five Bloch functions.

For the atomic wave functions the eigen functions in a cubic crystalline field were taken, *i.e.*

$$\begin{aligned}
&\varphi_1 = (15/4\pi)^{\frac{1}{2}}\, xy\, f(r)/r^2 && \varphi_2 = (15/4\pi)^{\frac{1}{2}}\, yz\, f(r)/r^2 \\
&\varphi_3 = (15/4\pi)^{\frac{1}{2}}\, zx\, f(r)/r^2 && \varphi_4 = (15/16\pi)^{\frac{1}{2}}\, (x^2 - y^2)\, f(r)/r^2 \\
&\varphi_5 = (5/16\pi)^{\frac{1}{2}}\, (2z^2 - x^2 - y^2)\, f(r)/r^2. &&
\end{aligned} \tag{5}$$

The matrix elements (4) can then be expressed in terms of the energy integrals between atomic functions and the wave vector **k**, and read [3])

$$\left.\begin{aligned}
&H_{11} = -\,4A_1 \cos\xi\cos\eta + 4A_2\cos\zeta\,(\cos\xi + \cos\eta) \\
&H_{22},\ H_{33} \text{ cycl.} \\
&H_{44} = 4A_4\cos\xi\cos\eta - 4A_5\cos\zeta\,(\cos\xi + \cos\eta) \\
&H_{55} = -\,(4/3)\,(A_4 + 4A_5)\cos\xi\cos\eta + (4/3)\,(2A_4 - A_5)\cos\zeta \\
&\qquad\qquad (\cos\xi + \cos\eta) \\
&H_{12} = -\,4A_3\sin\xi\sin\zeta \qquad H_{13},\ H_{23} \text{ cycl.} \\
&H_{14} = 0 \quad H_{24} = -\,4A_6\sin\eta\sin\zeta \qquad H_{34} = 4A_6\sin\xi\sin\zeta \\
&H_{15} = -\,(8/3^{\frac{1}{2}})\,A_6\sin\xi\sin\eta \qquad H_{25} = (4/3^{\frac{1}{2}})\,A_6\sin\eta\sin\zeta \\
&H_{35} = (4/3^{\frac{1}{2}})\,A_6\sin\xi\sin\zeta \qquad H_{45} = -\,(4/3^{\frac{1}{2}})\,(A_4 + A_5) \\
&\qquad\qquad \cos\zeta\,(\cos\xi - \cos\eta),
\end{aligned}\right\} \tag{6}$$

with $\xi = \frac{1}{2}ak_x$, $\eta = \frac{1}{2}\,ak_y$, $\zeta = \frac{1}{2}\,ak_z$ where a is the lattice parameter and

$$\left.\begin{aligned}
A_1 &= -\int \varphi_1(x,y,z)\, H_0^{(1)}\, \varphi_1(x - \tfrac{1}{2}a, y - \tfrac{1}{2}a, z)\, \mathrm{d}\tau \\
A_2 &= \int \varphi_1(x,y,z)\, H_0^{(1)}\, \varphi_1(x, y - \tfrac{1}{2}a, z - \tfrac{1}{2}a)\, \mathrm{d}\tau \\
A_3 &= \int \varphi_2(x,y,z)\, H_0^{(1)}\, \varphi_1(x - \tfrac{1}{2}a, y, z - \tfrac{1}{2}a)\, \mathrm{d}\tau \\
A_4 &= \int \varphi_4(x,y,z)\, H_0^{(1)}\, \varphi_4(x - \tfrac{1}{2}a, y - \tfrac{1}{2}a, z)\, \mathrm{d}\tau \\
A_5 &= -\int \varphi_4(x,y,z)\, H_0^{(1)}\, \varphi_4(x, y - \tfrac{1}{2}a, z - \tfrac{1}{2}a)\, \mathrm{d}\tau \\
A_6 &= \int \varphi_4(x,y,z)\, H_0^{(1)}\, \varphi_2(x, y - \tfrac{1}{2}a, z - \tfrac{1}{2}a)\, \mathrm{d}\tau
\end{aligned}\right\} \tag{7}$$

For the φ functions Fletcher[3]) used the atomic $3d$ functions of the Cu^+ ion, as calculated by Hartree and Hartree[5]). Its radial part could be approximated analytically by

$$f(r) = 85.88\, r^2\, e^{-5r} + 1.979\, r^2\, e^{-2r}. \tag{8}$$

The oscillatory part near the nucleus was not taken into account, being of minor importance for the integrals in (7). The effective potential in the free atom was approximated by

$$V(r) = -(1 + 28\, e^{-3r})/r. \tag{9}$$

Atomic units are used in these equations.

3. The perturbing potential

We shall now discuss what we have to take for the perturbing potential $H^{(1)}$ in (4) and (7). If we add other atoms to the central atom in order to form a lattice, one-electron potential troughs are added. These are not exactly equal to (9), since this corresponds to a coulombic potential at large distances. What we add actually are neutral atoms, so we may expect that in this approximation the extra potentials are given by

$$U(r) = -28\, e^{-3r}/r \tag{10}$$

centred around the additional lattice points. The consistent application of the band model should reveal that also the potential energy of the central atom is changed, since the charge of the electron under consideration is spread out over the whole crystal, and what an electron then feels in the centre is (10) and not (9). We should then find

$$H_0^{(1)} = 1/r - \Sigma_{n\neq 0}\, 28\, e^{-3|\mathbf{r}-\mathbf{r}_n|}/|\mathbf{r} - \mathbf{r}_n|. \tag{11}$$

We shall take only that value of $\mathbf{r}_n$ which coincides with that occurring in (7). In (11) no correlation between the positions of the electrons is taken into account. Actually, what we consider in (7) is the hopping of an electron of the central atom to one of its neighbours. Because of the correlation which exists between the positions of the electrons we may expect that in one atomic polyhedron two electrons of the same type are not present at the same time. We therefore assume that the perturbing potential is zero in the central atomic polyhedron and in the adjacent one is given by (10) with $\mathbf{r} \to \mathbf{r} - \mathbf{r}_n$. This way of taking correlation into account is quite similar to that which has been used by Wigner and Seitz[6]) in the cellular approximation, which gives good results. Fletcher used as perturbing potential $H^{(1)} = 0$ in the central polyhedron whereas its value at the neighbouring atom was given by (9). This is an over-estimation of the correlation effect, since it is equivalent to the assumption that the electron under con-

sideration keeps his brothers out of two polyhedra. We therefore repeated Fletcher's calculations and found that the contributions of the $1/r$ term and that of the screened Coulomb field in (9) are about the same, so that this reduces the results of Fletcher to about half their values, *i.e.* the bandwidth of 2.7 eV becomes 1.5 eV. Moreover we found it reasonable to treat the perturbing potentials caused by the two atoms under consideration on an equal footing, *i.e.* we assumed that each of them worked in the half of the whole space, with as boundary the plane bisecting perpendicularly the line joining the two lattice points. It turns out that all integrals are then about 50% larger than those of Fletcher, so that the total bandwidth is increased to 2.2 eV. This more or less arbitrary way of choosing the domain of integration can presumably introduce the most serious error in the calculation.

The values obtained for the integrals (7), expressed in eV, are compiled in table I.

TABLE I

Calculated values of the overlap energy integrals in eV for various assumptions of the perturbing potential

	$-28e^{-3r}/r$ (*a*)	$-1/r$ (*b*)	(*a*)—(*b*) (*c*)	(*a*) + (*b*) (*d*)	Fletcher (*e*)
$4A_1$	0.858	0.662	0.196	1.520	1.040
$4A_2$	0.238	0.204	0.034	0.442	0.309
$4A_3$	0.354	0.284	0.070	0.638	0.418
$4A_4$	0.591	0.488	0.103	1.079	0.727
$4A_5$	0.127	0.082	0.045	0.209	0.133
$4A_6$	0.373	0.293	0.080	0.666	0.465

We see that the two separate parts ((*a*) and (*b*)) of the potential used by Fletcher (*e*) give about the same, so that the difference (*c*) is about 1/9 of the sum (*d*), where (*d*) has to be compared with (*e*). This means that the use of Bloch functions without correlation (potential (11) corresponding to (*c*)) leads to a bandwidth of about 0.3 or 0.4 eV, this being far too small to have any physical significance. We shall use potential (10) corresponding to (*a*).

4. Interaction with the 4*s* electrons

Before plotting the $E - \mathbf{k}$ curves we have first to consider the interaction with the 4*s* electrons, which band overlaps the 3*d* band. The corresponding matrix elements are also given by (4) if φ_j is some type of located 4*s* function. Since the atomic 4*s* wave functions overlap very much at the actual distance of the atoms in the metal, it is not correct to use them for φ_0 (the index *o* is adopted for the 4*s* electrons). The 4*s* band is occupied by only 0.6 electrons per atom, so their wave functions closely resemble those of free electrons. If we are only interested in states not far above the Fermi level, we can put in

first approximation

$$\Sigma_n e^{i\mathbf{k}\mathbf{r}_n} \varphi_0 (\mathbf{r} - \mathbf{r}_n) \equiv \Omega^{-\frac{1}{2}} e^{i\mathbf{k}\mathbf{r}}, \tag{12}$$

Ω being the atomic volume. The matrix elements are then

$$H_{0d} = H_{d0}^* = \Omega^{-\frac{1}{2}} \int e^{-i\mathbf{k}\mathbf{r}} U(r) \varphi_d(\mathbf{r}) \, d\tau, \tag{13}$$

which, expressed in eV, are easily found to be:

$$\left.\begin{array}{ll} H_{01} = H_{10} = 0.380\, \xi\eta & H_{02} = H_{20} = 0.380\, \eta\zeta \\ H_{03} = H_{30} = 0.380\, \zeta\xi & H_{04} = H_{40} = 0.190\, (\xi^2 - \eta^2) \\ H_{05} = H_{50} = 0.110\, (2\zeta^2 - \xi^2 - \eta^2) & \end{array}\right\} \tag{14}$$

and with

$$H_{00} = 1.22\, (\xi^2 + \eta^2 + \zeta^2) - 5.27$$

if the zero of energy is taken at the Fermi level in the ferromagnetic state. Because of the use of the very simplified wave function (12) we may not expect that the results (14) give more than the order of magnitude. The symmetry in **k** space, however, is correct.

For wave vectors at or near the Brillouin zone boundaries, (14) is no longer valid. We may expect that at the top of the *s* band the wave functions have predominantly *p* character, which wave functions do not combine in these integrals with *d* functions, so we shall assume that the off-diagonal elements of (14) are zero at the Brillouin zone boundary in the first Brillouin zone.

The way in which the values in (14) go over into these zero values for the matrix elements depends of course on the periodic potential.

5. Solution of the secular equation

We have solved the secular equation for the (100) (110) and (111) orientation of the wave vector, and the results have been plotted in fig. 1, 2 and 3 respectively.

In the (100) direction the 4*s* functions combine with only one atomic 3*d* wave function with angular part $(2x^2 - y^2 - z^2)/r^2$. At the Fermi level their weight is about 25%, but the velocity is not much decreased.

The 4*s* electrons moving in the (110) direction combine with a hybride of the 3*d* functions with angular part xy/r^2 and $(2z^2 - x^2 - y^2)/r^2$. At the Fermi level the wave function has predominantly *d* character with a slightly increased velocity (about $\frac{1}{6}$ of that of a free electron with the same energy).

In the (111) direction there is a mixing of the 4*s* function with the 3*d* wave function having angular part $(xy + yz + zx)/r^2$. At the Fermi level the weight of the *d* electron wave functions is about 25%, but the velocity is nearly that of a free electron.

It is seen that in general the 4*s* electrons combine with *d* states which have maximum weight in the direction of propagation.

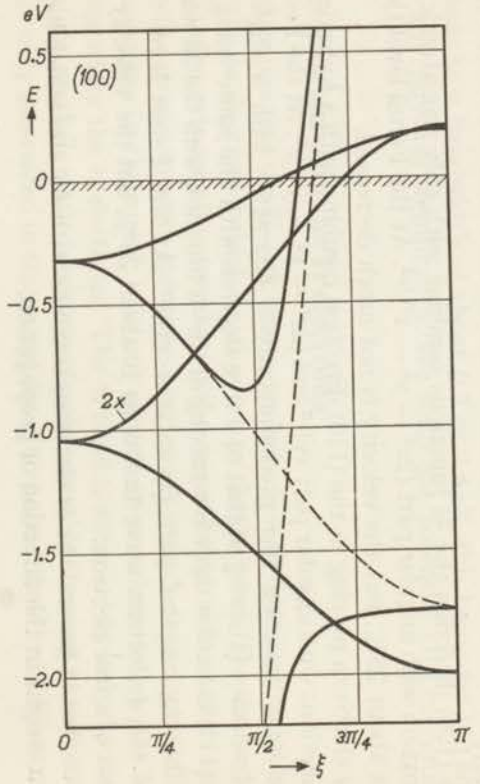

Fig. 1.

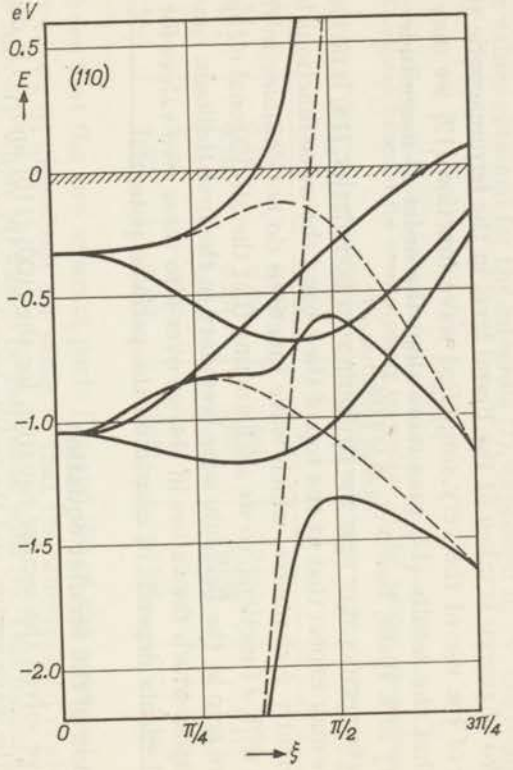

Fig. 2.

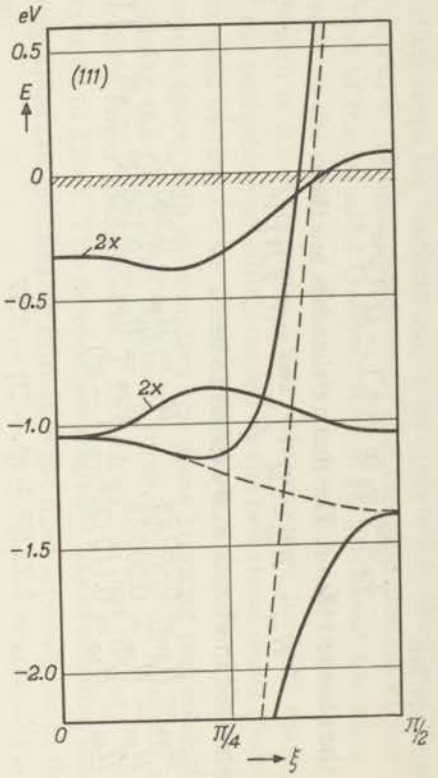

Fig. 3.

Energy *vs* wave vector curves for the (100), (110) and (111) orientations of k, respectively. The dashed curves are without s—d interaction. The Fermi level in the ferromagnetic state is at $E = 0$.

6. Discussion

We conclude that in the (100) and (111) orientations of the wave vector the 4*s* electrons near the Fermi level are not seriously affected. Their effective mass will be within a factor 2 of that of the free electron. It is to be expected that in general in all other orientations of the wave vector there will be a mixing of the *s* states and the wave functions belonging to the upper band. That is the $E - \mathbf{k}$ curves of the *s* functions and of the upper *d* band wave functions will repel each other. From the fact that this repulsion is zero in the (100) and the (111) direction, we conclude that an appreciable part of the electrons at the Fermi surface have nearly pure *s* wave functions in which the velocity and the effective mass are not substantially changed. Accordingly, for conduction problems *etc.* we have shown, that it is still possible to separate the electrons into two kinds, namely electrons with a normal mass, which carry most of the current, and the heavily-bound 3*d* electrons. The latter have, according to the figures 1, 2 and 3, a mass which is at least a

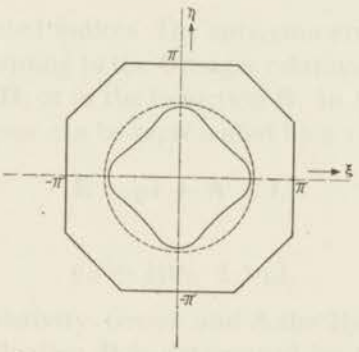

Fig. 4. Estimated Fermi surface of the conduction electrons for $k_z = 0$. Dashed circle: the same for free electrons.

factor 10 larger than that of the conduction electrons. We shall make use of this fact in chapter III. It follows, however, that the momenta of the conduction electrons no longer have spherical symmetry, as one would expect for a pure *s* band which is occupied by only 0.6 electrons per atom. In fig. 4 an estimated cut of the Fermi surface in a (100) plane in **k** space is plotted. This anisotropy will be of importance for the explanation of the relatively high magnetoresistance in nickel, as will be discussed in section 15.

Also, without calculating the exact shape of the density of states against energy curve, it is clear that it is changed substantially by the introduction of the 4*s* states into the calculation. This will therefore have a great influence on all the properties which are related to the band structure [7]).

Fletcher has calculated the complete band structure for states near the top of the band, and was able to construct the density of states curve in this energy range. From this the calculated the electronic specific

heat. We have not repeated these complete calculations for our modified interaction, since we believe that such calculations can only give an order of magnitude. This order of magnitude can also be obtained by putting the density of states at the Fermi level equal to the average level density. We then find for a band width or 2.2 eV for the coefficient γ from the expression $c_v = \gamma T$, $\gamma = 1.3 \times 10^{-3}$ cal mol^{-1} deg^{-2}, as compared with an observed value of 1.7×10^{-3}.

Our conclusion is that for the actual multi-electron wave function a continuum of energy levels above the lowest state exists, due to an increase in kinetic energy of the 3*d* electrons. The essential features of this continuum may be calculated using the one-electron Bloch functions, provided the correlation is taken into account.

CHAPTER II

THE HALL EFFECT IN FERROMAGNETIC METALS AND ALLOYS

7. Introduction

The linear relationship between the current density **i** and the electric field **E** in a conductor can be described by a tensor w according to

$$E_i = w_{ij}\, i_j , \tag{1}$$

summed up over repeated indices. The antisymmetrical part of this tensor, *i.e.* $\frac{1}{2}(w_{ij} - w_{ji})$, is, according to the Onsager relations, odd in the externally applied magnetic field **H**, or in the induction **B**. In three dimensional space an antisymmetrical tensor can be represented by a vector. We then have

$$\mathbf{E} = \varrho\,\mathbf{i} + \mathbf{A} \times \mathbf{i},$$

where ϱ, defined by

$$\varrho_{ij} = \tfrac{1}{2}(w_{ij} + w_{ji}),$$

is the symmetrical resistivity tensor and **A** the Hall vector. The relation between **A** and the induction **B** is determined by the material only. If a linear relationship exists, which usually will be a sufficient approximation, this relation is described by a tensor

$$A_i = R_{ij}\, B_j. \tag{2}$$

The tensor R_{ij} has the symmetry of the crystal. For a cubic crystal such a tensor has to be isotropic, *i.e.* it is diagonal with three equal diagonal matrix elements R_0. This constant is the Hall coefficient obeying

$$E_y = R_0\, i_x\, B_z , \tag{3}$$

if the primary current is in the x direction and **B** along the z axis. This Hall tension is a consequence of the Lorentz force acting on the moving electrons. For free electrons R_0 is then equal to

$$R_0 = (Nec)^{-1}, \tag{4}$$

where Ne is the total amount of moving charge per cm³. If the electrons are not free N should be replaced by N_{eff}, the effective number of charge

carriers. If the sign is found to be opposite, we say that the effective charge of the carrier is $+|e|$ so that we have conduction by holes. Assuming that these quantities do not change with temperature, R_0 should be independent of temperature. For most metals this is essentially true. For monovalent metals one finds that N corresponds to about one electron per atom, as one would expect.

For the ferromagnetic materials it is found that $\mathbf{A}$ is not proportional to $\mathbf{B}$, but that a constant part has to be added [8]). This "spontaneous" part, as we shall call it, is caused by the spontaneous magnetization $\mathbf{M}_s$. In this case we cannot speak of a linear relationship between $\mathbf{A}_s$ and $\mathbf{M}_s$, since the magnitude of $\mathbf{M}_s$ cannot be changed. Therefore even for a cubic crystal the dependence of this spontaneous part $\mathbf{A}_s$ on $\mathbf{M}_s$ can only be described by an approximate relationship, which contains more than one constant. If we denote the direction cosines of $\mathbf{M}_s$ with respect to the cubic axes by α_i, we get for the components A_{si} of $\mathbf{A}_s$ along these axes in first approximation

$$A_{si} = 4\pi R_s M_{si} \{1 + p\,\alpha_i^2 + q\,\alpha_i^4 + r\,(\alpha_2^2\alpha_3^2 + \alpha_3^2\alpha_1^2 + \alpha_1^2\alpha_2^2)\} + \ldots\} \quad (5)$$

The occurrence of the constants p, q and r makes the effect anisotropic. The only measurements made on single crystals are those of Webster [9]) on iron which showed that the effect is isotropic. In a polycrystalline material, which is being magnetized, the resultant $\mathbf{A}_s$ will have a mean value of (5) as is found by averaging over all Weiss domains, assuming that the current is homogeneous. For finite values of p, q, r, this average will take different relative values at different stages of the magnetization process. In that case $\mathbf{A}_s$ will not be proportional to the resultant magnetization. In the measurements on polycrystalline samples we never found a marked deviation of proportionality between the Hall voltage and the applied field well below saturation, *i.e.* as long as the magnetization is linear in the applied field. We therefore conclude that the terms p, q and r are not predominant and may be neglected, so that for ferromagnetic materials

$$E_y = (R_0 B_z + 4\pi R_s M_z)\, i_x. \quad (6)$$

Because we have dropped the non-linear terms in the direction cosines it may be expected that (6) also holds in the paramagnetic region as for instance near the Curie point [10]) or in strongly paramagnetic substances [11]). Since in this case both $\mathbf{B}$ and $\mathbf{M}$ are proportional to $\mathbf{H}$, one observes this anomalous Hall effect as a normal one. For substances with a paramagnetic susceptibility of the usual order of magnitude, the contribution of this anomalous effect is negligible. It is then also immaterial whether we use in (3) $\mathbf{B}$ or $\mathbf{H}$. For ferromagnetic materials, because we add a term proportional to $4\pi\,\mathbf{M}$, it is again possible to use $\mathbf{H}$ instead of $\mathbf{B}$. We prefer the use of this last quantity since this is the mean magnetic field inside the crystal. This choice will be justified theoretically and experimentally in the next sections.

The spontaneous Hall effect is usually very large, *i.e.* $R_s \gg R_0$. For nickel at room temperature for instance $R_s \approx 10\, R_0$. An extra magnetic field of magnitude $(R_s/R_0)\, 4\pi M$ would give the same effect, which is in this case about 60.000 oersted. Although such an effective field gives a good idea of the order of magnitude we do not consider it to be a good description of the effect: it will appear from the experimental results that at different temperatures R_s and R_0 are quite uncorrelated, whereas R_s is a monotonic function of temperature. Besides the large magnitude, its strong increase with increasing temperature is the most striking feature of this Hall effect. Earlier experiments [12]) seemed to indicate that for nickel at low temperatures $R_s \approx R_0$, whereas at room temperature $R_s \approx 10\, R_0$. In 1910 Smith [13]) [8]) showed that above room temperature R_s increases strongly. In particular at low temperatures this behaviour cannot be understood in terms of a variation of the magnetic properties: the spontaneous magnetization does not increase more than 5% below room temperature. The only relevant property of the material, which changes in a similar way, is its electrical resistivity. If a relationship between R_s and ϱ exists, one should expect that for disordered alloys R_s decreases much less below room temperature than it does for the pure metals. Starting from this idea Dr J. Volger and the author measured R_s of a number of alloys at temperatures of liquid hydrogen, of liquid nitrogen and at room temperature. In most cases it was found that R_s and ϱ have a similar temperature dependence. We also measured some nickel samples, and it was found that for the purest material R_s goes to zero for $T = 0$. We may therefore state that R_s is correlated with the electrical resistivity of the material.

As to the theoretical aspect of the problem we could prove by an extension of Houstons proof, which states that a periodic lattice has no resistivity, that R_s must also be zero in such a lattice. This is in agreement with our experimental results obtained with very pure nickel. We shall show in this chapter that the spontaneous Hall effect must be caused by skew scattering due to spin-orbit interaction of the magnetized electrons on the imperfections of the lattice.

8. Experimental data

The Hall effect was determined for a number of nickel alloys both with magnetic ions like iron or cobalt as second component and with non-magnetic ions. Measurements were carried out at room temperature and at the temperatures of liquid nitrogen and hydrogen in fields up to 14000 oersted. The samples were in the form of thin foils with dimensions $50 \times 10 \times 0.05$ mm^3. The Hall contacts were Ni wires of 50μ thickness which were spot welded on the edges of the specimen over a distance which did not exceed 0.5 mm. At one side two contacts were made at 1 cm apart and were overbridged by a potentiometer. In this way it is possible [14]) to measure the

pure Hall voltage. At this stage the specimens were annealed for one hour at 1000°C in purified hydrogen, after that slowly cooled to 600°C and then pulled out into the cold part of the tube. The current leads were soldered on the specimen.

The finite dimensions of the specimen cause some errors in the measurement of the Hall effect. This has been investigated by Volger and Frank [15]) and for our case the maximum error is $1\frac{1}{2}\%$. Another cause for error is in the fact that the Ni wire of the Hall contacts short circuits to some extent the Hall voltage over the distance over which it is welded on the foil. If the effective resistance of that part of the foil is R_1 and that of the wire R_2, the Hall voltage over that part is reduced by a factor $R_2/(R_1 + R_2)$. If we assume that for R_1 we have to take a part of the foil with a width of the order of the length of overlapping, we find, if the wire and the foil have the same specific resistivity, a maximum error of 1%. For the measurements on alloys at low temperatures it would be better to take for the material of the wire also an alloy, but this gave difficulties with the welding.

The current through the sample was 1 — 3 A and the Hall voltage was compensated with a Dieselhorst compensator. Every point was measured four times, *i.e.* both the current and the magnetic field were commuted in order to find that part of the voltage which is odd in both the current and the field. The field was always first brought to its maximum value and after that to the desired one, in order to avoid hysteresis. A few typical curves are shown in fig. 5. The results are given in table II. The magnetization has only been measured at 77° and 290°K. The value at 20° is estimated. The spontaneous Hall angle has been corrected for the change of the magnetization. We see that it is mostly of the order of 10^{-2}. For the purest Ni specimen the spontaneous Hall effect goes to zero at the lowest temperature, as is also seen from fig. 5. This is not the case for the impure samples [12]) and the alloys. Also the "pseudo nickels" (Ni-Fe-Cu alloys) have a finite R_s at $T = 0$. The material of the specimens quoted as "annealed" and "hard" is not as pure as the carbonyl nickel. In this case R_s increases upon annealing.

The normal Hall coefficient of the commercial Ni behaves as one should expect: it is constant as a function of temperature. For the purer specimens this is not the case, R_0 increases appreciably for increasing temperature. Also the R_0 of some Ni-Co alloys do not agree with measurements at room temperature of other authors [16]), so we conclude that the Hall effect in ferromagnetic metals and alloys is extremely sensitive to impurities. It appears from the experimental results that R_0 and R_s are not closely correlated. This is most clearly demonstrated for the Ni alloys with non-magnetic ions where R_0 varies quite irregularly with temperature, whereas R_s is a monotonic function of the resistivity. Pugh [17]) has recently discussed theo-

retically R_0 for Ni and Ni-Cu alloys and could explain why there R_0 decreases with increasing temperature. For quite a number of alloys and for nickel, however, the reverse is true, so his argument cannot be considered as conclusive. The high value of R_0 of the V alloy at room temperature is

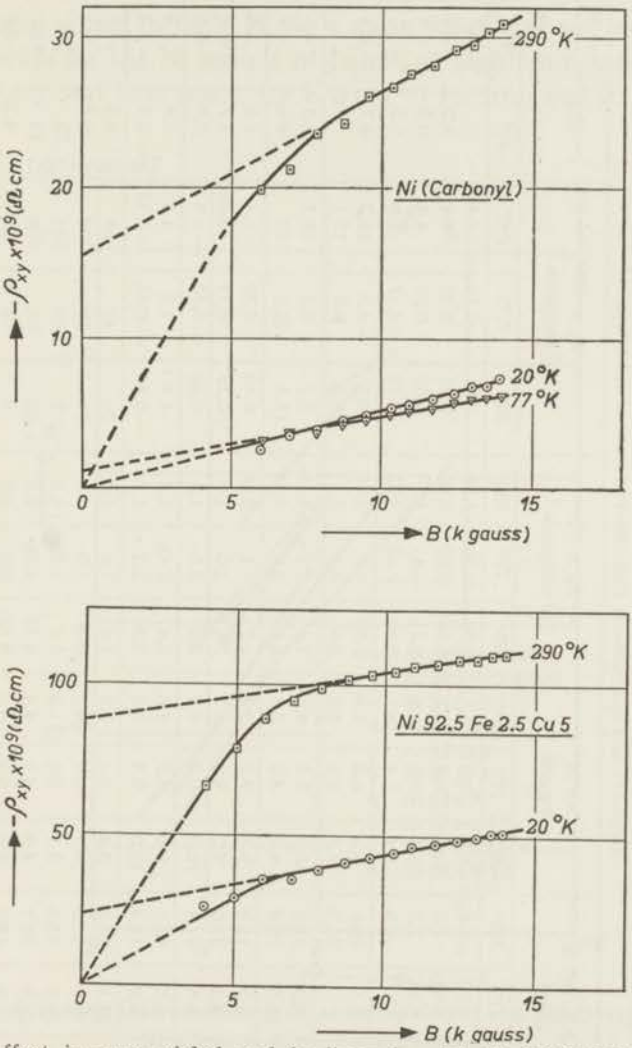

Fig. 5. Hall effect in pure nickel and in "pseudo nickel" (Ni 92.5 Fe 2.5 Cu 5) at different temperatures. Extrapolation of the high field values to $B = 0$ gives the spontaneous contribution. This is zero for the Ni sample at 20°K. Note the different scales for the two specimens.

spurious, and is due to the high intrinsic permeability near its Curie point. This possibility was first suggested by Rostoker and Pugh[10]). In this paper we shall further only discuss R_s.

TABLE II

Ordinary and spontaneous Hall effect of some nickel alloys.

Composition atomic %	$\varrho \times 10^6$ Ω cm			$4\pi M$ k gauss			$-R_0 \times 10^{12}$ Ω cm/gauss			$-R_s \times 10^{12}$ Ω cm/gauss			$-\varphi_{SH} = \frac{-R_s \cdot 4\pi M_0}{\varrho} \times 10^3$			n
	20°	77°	290°	20°	77°	290°	20°	77°	290°	20°	77°	290°	20°	77°	290°	
Ni (carbonyl)	0.059	0.69	6.8	6.4	6.4	6.1	0.50	0.36	1.26	0.0	0.19	2.4		1.7	2.3	
Ni (commercial)	0.40	0.86	7.2	6.4	6.4	6.1	0.58	0.52	0.60	0.25	0.27	6.4	4.0	2.0	5.5	
Ni (hard)	0.32	0.84	7.1	6.4	6.4	6.1	0.51	0.51	1.1	0.05	0.05	4.4	0.9	0.4	3.9	
(annealed)	0.12		6.9	6.4	6.4	6.1	0.40	0.42	1.33	0.15	0.17	3.6	8.3		3.3	
Ni 92.5 Fe 2.5 Cu 5	6.3	7.1	15.0	6.2	6.2	5.9	2.05	1.7	1.45	3.7	4.2	15.2	3.7	3.8	6.2	1.7
Ni 85 Fe 5 Cu 10			20.2	6.1	6.1	5.8	2.4	2.1	2.1	3.9	4.8	13.1			3.9	
Ni 91 Cu 9	8.3	9.3	18.5	5.1	5.1	4.8	2.4	2.1	1.15	7.2	8.2	27.7	4.5	4.5	7.7	1.7
Ni 82 Cu 18	15.5	16.7	28.8	4.1	4.0	3.6	2.5	2.3	1.35	17.5	20.0	44	4.6	4.9	6.3	1.4
Ni 90 Co 10	2.2	2.3	11.8	7.7	7.7	7.4	1.2	1.1	2.25	0.48	0.77	7.4	1.8	2.6	4.8	
Ni 80 Co 20	3.2	3.3	12.0	9.0	9.0	8.7	2.1	2.0	1.9	0.27	0.14	0.65	0.7	0.4	0.5	
Ni 70 Co 30	3.9	4.0	11.4	10.2	10.2	9.9	2.9	2.8	1.3	0.32	— 0.53	— 1.9	0.8	— 0.6	— 1.7	
Ni 89.3 Fe 10.7	3.8	4.5	13.1	9.0	9.0	8.6	0.4	0.45	1.7	1.4	1.2	1.8	3.4	2.5	1.2	
Ni 84 Fe 16	4.6	5.2	14.4	10.0	9.9	9.5	2.35	2.2	1.7	— 0.40	— 0.65	— 0.95	— 0.9	— 1.2	— 0.7	
Ni 92 Al 8	12.4	13.1	24.8	3.2	3.1	2.6	1.8	1.8	1.0	36	42	85	9.3	10.1	10.9	1.2
Ni 97 Si 3	9.5	10.1	18.0	4.9	4.9	4.7	0.7	1.0	1.1	18	19	39	9.2	9.1	10.6	1.2
Ni 93 V 7	33.2	34.1	43.9	3.1	2.8	1.3	1.6	1.95	4.8	237	255	221	22	23	16	
Ni 97 Mo 3	20.9	21.9	30.7	4.8	4.7	4.1	1.15	1.05	1.5	83	84	106	19	18	16	0.6
Ni 97 Sn 3	10.8	11.4	17.2	5.0	5.0	4.6	0.85	0.9	2.0	18	18	34	8.3	8.0	10.2	1.4
Ni 98.4 W 1.6	11.0	11.9	19.6	5.9	5.8	5.4	0.7	1.05	1.1	20.3	21	39.6	10.7	10.6	11.8	1.2

As already noted, especially for the alloys with a non-magnetic element, R_s changes monotonically with ϱ. This is demonstrated in fig. 6. From the slope we find the power n of the relation

$$R_s \sim \varrho^n$$

which has been added to table II. As a mean value we have $n \approx 1.4$, which value also holds for the Ni sample of Jan[18]) at high temperatures. Such a graph of $R_s vs \varrho$ was first made by Kooy[19]) for iron and its alloys with silicon.

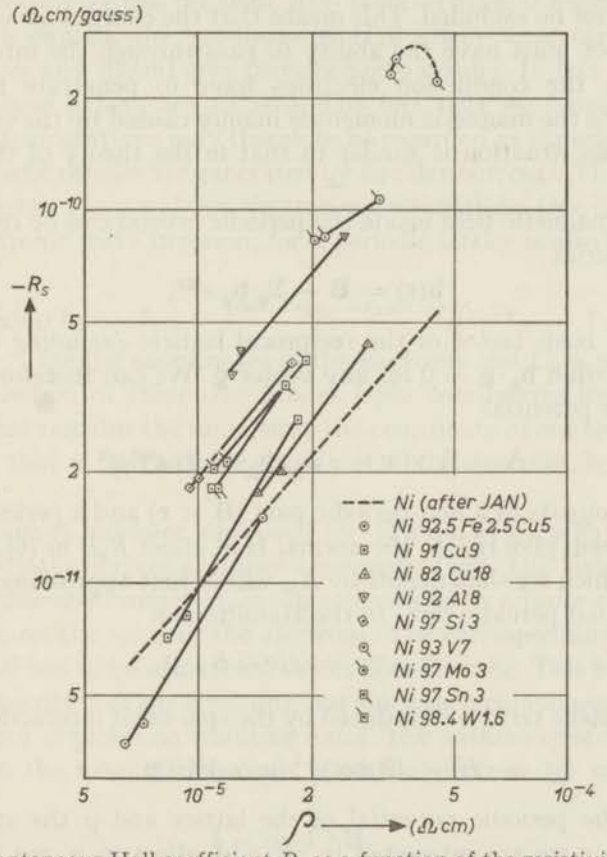

Fig. 6. The spontaneous Hall coefficient R_s as a function of the resistivity ϱ for several Ni alloys at three temperatures.

For nickel R_s is negative. The addition of Co or Fe decreases the absolute value of R_s, so that it passes through zero at about 25% Co or 15% Fe. For pure Co and Fe R_s is positive[16]). It is remarkable that these zero points occur at about the same Bohr magneton number ($n_B \approx 0.9$). The normal Hall coefficient R_0 has still the same sign as that of Ni, but for pure iron it is also positive[16]) (hole conduction).

9. Theory for a periodic lattice

Three possible causes for the spontaneous Hall effect might be:

a) Magnetic fields originating from the dipoles;

b) Spin-orbit interaction;

c) Inhomogeneous magnetic fields caused by the electrical current i_x through the crystal.

The mean field averaged over the whole space of the crystal is equal to **B**. If we assume that this field acts on the electrons which carry the current, then the space within the circular currents, which generate the magnetic dipole, may not be excluded. This means that the charge carriers which give the Hall effect must have the ability to pass through the interior of these currents, *i.e.* the conduction electrons have to penetrate the magnetic electrons since the magnetic moment is mainly caused by the spins of the 3*d* electrons. This situation is similar to that in the theory of the hyper-fine splitting.

The total magnetic field inside the periodic crystal can be represented by the Fourier series

$$\mathbf{h}(\mathbf{r}) = \mathbf{B} + \Sigma_{\mathbf{g}}\, \mathbf{b}_{\mathbf{g}}\, e^{i\mathbf{g}\mathbf{r}},$$

where $\mathbf{g}$ is a basis factor of the reciprocal lattice, excluding $\mathbf{g} = 0$. Since div $\mathbf{h} = 0$, we find $\mathbf{b}_{\mathbf{g}} \cdot \mathbf{g} = 0$ for any vector $\mathbf{g}$. We can therefore derive $\mathbf{h}(\mathbf{r})$ from a vector potential

$$\mathbf{A} = \mathbf{B} \times \mathbf{r} + i\, \Sigma_{\mathbf{g}}\, (\mathbf{b}_{\mathbf{g}} \times \mathbf{g})\, e^{i\mathbf{g}\mathbf{r}}/g^2, \tag{7}$$

which then consists of a non-periodic part $(\mathbf{B} \times \mathbf{r})$ and a periodic part. The part with **B** will give rise to the normal Hall effect $R_0 B$ in (6). The second part of (7), which we shall denote by $\mathbf{A}_p$, will in first approximation give rise to an additional periodic term in the Hamiltonian

$$H_{dip} = -\,(e/mc)\, \mathbf{A}_p \cdot \mathbf{p}. \tag{8}$$

A similar periodic term is introduced by the spin-orbit interaction [20])

$$H' = (2\, mec)^{-1}\, (\boldsymbol{\mu} \times VV)\, \mathbf{p}, \tag{9}$$

where V is the periodic potential of the lattice and $\boldsymbol{\mu}$ the spin magnetic moment. Since we are interested in an odd effect in $\boldsymbol{\mu}$, we have only to consider its diagonal elements, so we can treat it as being a number. The effects *a*) and *b*) thus give rise to periodic potentials. The resulting Hamiltonian without the effect of **B** is still periodic and the solutions of the Schroedinger equation will be of the Bloch type. Electrons in these states can carry a translational current which is thus stationary, *i.e.* no acceleration results, and no field strength is needed to maintain this current, so that $R_s = 0$. The conduction electrons simply report the space averaged field in the metal. This is independent of the charge distribution of these electrons in space, so

it is immaterial whether the electrons avoid places of high field strength or not. The inhomogeneous part of the field and the inhomogeneous charge distribution have no influence on the effective magnetic field because of their periodicity. W a n n i e r [21]) and before him other authors have treated this problem of the dipole fields and found fields different from **B**. Their field was in first approximation given by $\mathbf{H} + 2\pi\,\mathbf{M}(1 + p)$ where p measures the relative probability of a conduction electron penetrating into the interior of a polarized electron. In this case $p \approx 0$, so $\mathbf{H}_{eff} \approx 2\pi\,\mathbf{M}$. These authors did not take into account the periodicity of the lattice and their analysis is therefore irrelevant for this problem. Also theories using the spin-orbit interaction [22]) [8]) to explain the spontaneous Hall effect were carried out for periodic lattices and should give therefore zero results. In fact the relevant integrals in these papers are all zero. The fact that we found $R_s = 0$ for nickel at low temperatures may therefore be regarded as experimental proof that the magnetic dipoles are generated by circular currents. This conclusion is not restricted by the use of one-electron wave functions. One can show that the total electronic wave function, for a periodic lattice is also of the Bloch type, *i.e.*

$$\Psi_{\mathbf{k}}(\mathbf{r}_1, \mathbf{r}_2 \ldots \mathbf{r}_N) = e^{i\mathbf{k}(\mathbf{r}_1+\mathbf{r}_2+\ldots+\mathbf{r}_N)/N}\, U_{\mathbf{k}}(\mathbf{r}_1, \mathbf{r}_2 \ldots \mathbf{r}_N),$$

where $\mathbf{r}_1, \mathbf{r}_2 \ldots$ are the coordinates of the electrons and $U_{\mathbf{k}}$ a periodic antisymmetric function of these coordinates (spin coordinates included). The above argument remains the same, only the coordinate of one single electron is replaced by that of the centre of gravity of all the electrons, but this is just what we need.

The last point *c*) has been discussed by R u d n i t s k y [23]) and also in ref. [8]). The primary current i_x causes a magnetic field. This field, which has not yet been discussed under *a*), is inhomogeneous in a finite crystal and a force is acting on the spins of the electrons. The corresponding part of the Hamiltonian H has to be subtracted before H is periodic. This force will also try to curve the paths of the electrons, but since each component of the field averages to zero, it yields no resulting e.m.f. The authors quoted calculated the force **f** on the magnetic moment $\boldsymbol{\mu}$ of the electron by means of the equation

$$\mathbf{f} = (\boldsymbol{\mu} \cdot \nabla)\,\mathbf{H}. \qquad (10a)$$

This equation only applies to dumb-bell dipoles. The adequate force equation for dipoles generated by circular currents is

$$\mathbf{f} = \nabla(\boldsymbol{\mu} \cdot \mathbf{H}). \qquad (10b)$$

Equation (10*a*) is clear: we must have the change of **H** in the direction of $\boldsymbol{\mu}$. That (10*b*) applies to circular currents follows most directly by writing down the relation between the magnetic moment density **m** and the dipole current density **i**:

$$\text{curl}\ \mathbf{m} = \mathbf{i}/c.$$

The Lorentz force per unit volume $\mathbf{f}_I$ is given by $-\mathbf{H} \times \mathbf{i}/c$ so that we get

$$\mathbf{f}_I = -\mathbf{H} \times \text{curl}\, \mathbf{m} = -\nabla(\mathbf{m}\cdot\mathbf{H}) + (\mathbf{H}\cdot\nabla)\,\mathbf{m}, \qquad (10c)$$

where only $\mathbf{m}$ is differentiated. Integrating (10*c*) in order to find the total force, we find for the last term $-\int \mathbf{m}\cdot\nabla\mathbf{H}\, d\tau = 0$. The first term gives in the same way, assuming that the gradient of $\mathbf{H}$ is constant over the volume of the dipole, the equation (10*b*), where $\boldsymbol{\mu} = \int \mathbf{m}\, d\tau$. Though $\mathbf{m}$ is not uniquely defined by its curl, the gradient field which can be added does not contribute to $\boldsymbol{\mu}$. The difference between (10*a*) and (10*b*) is $\boldsymbol{\mu} \times \text{curl}\, \mathbf{H}$ and is zero when there are no currents. In our case $\mathbf{H}$ is generated by the currents within the sample and therefore only (10*b*) is valid. But this force, being a macroscopic gradient field, cannot give an e.m.f. in a closed circuit. We conclude therefore that in a periodic crystal no spontaneous Hall e.m.f. can exist, *i.e.* $R_s = 0$.

It may be noted that (10*a*) gives rise to a Hall effect of the required form as was derived by the authors quoted. The effect is given by

$$\boldsymbol{\mu} \times \text{curl}\, \mathbf{H} = \boldsymbol{\mu} \times 4\pi\, \mathbf{i}/c,$$

where $\mathbf{i}$ is the primary current. The force is then equal to

$$\mathbf{f} = 4\pi\, \boldsymbol{\mu} \times \mathbf{i}/c,$$

corresponding to a field strength of

$$\mathbf{E} = 4\pi\, \mathbf{M} \times \mathbf{i}/Nec,$$

where N is the net number of Bohr-magnetons per unit volume. According to (4) this equation is equivalent to the normal Hall effect formula with an effective field of $4\pi\, \mathbf{M}$, if it is assumed that only the magnetized electrons carry the current. For rod shaped dumb-bell dipoles we should have found that the space averaged field is equal to $\mathbf{H}$ instead of $\mathbf{B}$, but now the missing $4\pi\, \mathbf{M}$ is given by the effect *c*), so that we again arrive at an effective field equal to $\mathbf{B}$ in a periodic lattice. In actual ferromagnetics, however, as we have seen in chapter I, the current is presumably carried for the greater part by the unmagnetized *s* electrons, so the last reasoning breaks down.

10. Combined influence of spin-orbit interaction and an applied electric field

In order to maintain a stationary current in an imperfect crystal one has to apply an electric field. In this section we shall discuss the combined influence of such a uniform electric field and the spin-orbit interaction on the wave functions, but still neglecting the perturbations of the lattice. The wave functions are therefore still of the Bloch type. Such a procedure has also been followed by Karplus and Luttinger[24]) (K—L paper) and these authors claimed to show that as a result a stationary current is

generated, being proportional and perpendicular to both the applied field and the magnetization, thus having the symmetry of a Hall current. The constant of proportionality is in first approximation independent of temperature, so that $R_s \sim \varrho^2$, which dependence on ϱ agrees quite well with the experimental data, this being also the case with the order of magnitude of the constant of proportionality. We shall show that this effect is spurious, and that in the stationary state it is compensated exactly by the opposite action of the collisions of the electrons against the perturbing potentials.

Prior to a discussion of this matter we shall treat the spin-orbit interaction in more detail. Since one can write a triple scalar product in different ways, it is also possible to identify (9) as a result of the action of a magnetic field

$$\mathbf{H}_{s.o.} = (\mathbf{p} \times \nabla V)/2\,mec = -\tfrac{1}{2}(\mathbf{v}/c) \times \mathbf{E} \qquad (9a)$$

on the spin magnetic moment $\boldsymbol{\mu}$. The fine structure of spectra is caused by the fact that the spin can be either parallel or antiparallel to this spin-orbit magnetic field. For the present problem we shall be interested in the fact that this $\mathbf{H}_{s.o.}$ is inhomogeneous, due to the inhomogeneity of V, so that the electron feels a force *via* its spin magnetic moment. The nature of this force can be seen most easily by writing (9) in a third way:

$$H' = (2mc)^{-1}\,\mathbf{E}\,(\boldsymbol{\mu} \times \mathbf{p}),$$

showing that the spin-orbit interaction also can be interpreted as the interaction of an electric dipole moment with an electric field. So a moving electron has for an observer in a system at rest an electric dipole moment

$$\boldsymbol{\mu}_e = -\tfrac{1}{2}(\mathbf{v}/c) \times \boldsymbol{\mu}. \qquad (9b)$$

For an electron moving in the x direction with its spin along the z axis this polarization points in the y direction, so that the energy is $E_y\,\mu_z\,v_x/2c$. In a crystal with potential troughs at the ion sites it means that the "potential energy" for the travelling electron is smaller if it passes the ions on the right than on the left. As a result the charge density will become asymmetrical with respect to the ions, so that a finite polarization in the y direction, or more generally perpendicular to the velocity and to the spin, will result, which changes sign with v_x and μ_z. The altered wave function is still of the Bloch type. The situation has been plotted schematically in fig. 7. In the lowest figure, which refers to the $\mathbf{k}$ space, this polarization of the wave functions (referring to normal space) has been indicated.

An applied uniform electric field $E_x = F$ has two effects:

a) The orientation effect

Electrons moving in the y direction have opposite polarization in the x direction ($\pm q_x$) for opposite values of k_y. The energies for the two states in the field are therefore changed by an amount of $\mp eFq_x$ respectively, so that

$E(k_y) \neq E(-k_y)$. We can say that the field tries to orient the permanent dipole moments. The velocity in the y direction in the state characterized by $\mathbf{k}$ is $\hbar^{-1}\,\partial E/\partial k_y$. Usually $E(\mathbf{k}) = E(-\mathbf{k})$, so that an electron in the state $\mathbf{k}$ compensates exactly the drift of one in the state $-\mathbf{k}$. Let us assume with K—L that the density function is a function of the energy of the individual states: $\varrho = \varrho(E)$. In that case the resultant velocity is obviously zero for the case of $E(\mathbf{k}) = E(-\mathbf{k})$. In our case $E(\mathbf{k}) \neq E(-\mathbf{k})$, so this simple argument does not apply. The total velocity in the y direction, however, is proportional to

$$\langle v_y \rangle \sim \iint \mathrm{d}k_x\,\mathrm{d}k_z \int (\partial E/\partial k_y)\,\varrho(E)\,\mathrm{d}k_y \tag{11}$$

and is zero, since the last integral can be reduced to one with respect to E. In fact many electrons with small velocity compensate the opposite current of less electrons with larger velocity. So we can state that any band, even if

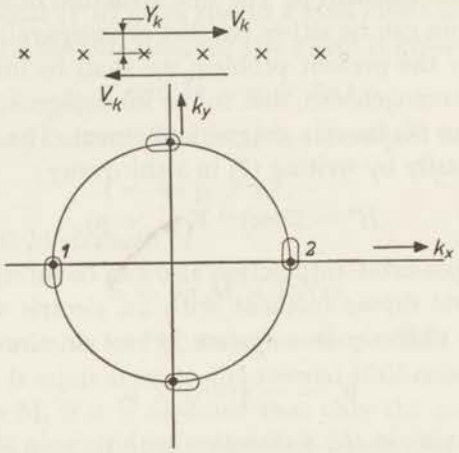

Fig. 7. Schematic plot of the effect of polarization caused by the spin-orbit interaction on travelling electrons. The upper figure is in normal space, the crosses indicate the ions, and the lower figure is in wave vector space. The ellipses indicate the direction of the polarization.

it is asymmetrical, does not carry a current if it is filled up with a density which is a function of the energy only. This fact was also recognized by K—L, as is borne out by their eq. (2.13).

b) The acceleration

Secondly the electric field accelerates the electrons, *i.e.* transitions between states with different k_x occur, so that for instance in effect an electron in state 1 (see fig. 7) at one side of the Fermi surface changes to state 2 at the other side, thereby changing the crystal momentum with $\hbar(k_{2x} - k_{1x})$. But at the same time there is a shift in position in the y direction equal to $2q_y$. Thus an acceleration in the x direction gives rise to a velocity in the y direction. This effect has been considered in the K—L paper and we get their

result (2.19) at once by putting $\partial\varrho/\partial t$ of the equation $v_y = (\partial\varrho/\partial t)\, q_y$, where q_y is identical with $i\, J_a(\mathbf{k})$ of their eq. (2.6), equal to

$$(\partial\varrho/\partial t)_{field} = -\,(\partial\varrho/\partial E)\,.\,(\partial E/\partial k_x)\,.\,eF/\hbar.$$

In reality there is in the equilibrium state no resultant change of the density matrix, since we have

$$\partial\varrho/\partial t = (\partial\varrho/\partial t)_{field} + (\partial\varrho/\partial t)_{coll} = 0,$$

so in the steady state the effect of the applied field is cancelled exactly by that of the collisions.

The only result is a constant polarization in the y direction P_y proportional to i_x caused by the shift of the Fermi sphere in the x direction. In a finite specimen this gives a depolarizing field which is in an ellipsoid equal to $E_y = -N_y P_y$, with N_y the demagnetization coefficient, which is here a depolarization coefficient. This field is curl free, so it cannot give an e.m.f. in a closed circuit, *i.e.* it does not contribute to R_s.

One might think for a moment that the occurrence of a field E_y is not in agreement with our previous statement that in a periodic crystal no field can be generated. The solution is that in the last case E_y is only a consequence of the finite dimensions of the crystal and such a crystal cannot be considered as being perfectly periodic.

The K–L reasoning can be made more similar to ours by not splitting in their eq. (2.12) H_T into $H_T = H + H'' = H_p + H'' - H_1''$, but into $H_T = H_p + H_i''$. Then no interband matrix elements enter, since H_i'' connects only states within one band. Their conclusion following eq. (2.19) may therefore not be very relevant. In fact therefore K–L calculated the current in an accelerated system of electrons. This originates from the fact that they used in their eq. (2.12) H_T instead of H_p.

We shall now put the analysis in a more rigourous form. The electric field F gives an additional term in the Hamiltonian

$$H'' = -\,eFx.$$

This potential has matrix elements between Bloch functions with the same $\mathbf{k}$, so it contains a periodic part. This is a saw-tooth-like potential, which is in the l'th atomic cell defined by

$$(H_i'')_l = -\,eF\,(x - x_l),$$

where x_l is the x coordinate of the centre of the l'th cell. The remaining part is a staircase-like potential, being in the same cell given by

$$(H_s'')_l = -\,eFx_l,$$

which has no matrix elements between Bloch functions with the same $\mathbf{k}$, provided we choose the origin of the coordinate system in the centre of

gravity of the crystal. Since the electron cannot distinguish between the periodic potential H_t'' induced by the applied field and a similar one if it were caused by the ions, we shall assume that the total periodic Hamiltonian, which determines the Bloch functions, is given by

$$H_p = H + H_t''. \tag{12}$$

It may be noted that our H_p is different from that used by K–L. In (12) H is the periodic Hamiltonian which includes the spin-orbit interaction H' of (9). The total Hamiltonian is given by

$$H_T = H_p + H_s''. \tag{13}$$

We shall now calculate the behaviour of a wave packet of Bloch functions within one band:

$$\psi(\mathbf{r}, t) = \Sigma_{\mathbf{k}}\, a(\mathbf{k}, t)\, \varphi(\mathbf{k}, \mathbf{r}) \tag{14}$$

under the action of the total Hamiltonian (13), where the $\varphi_{\mathbf{k}}$ satisfy

$$H_p\, \varphi_{\mathbf{k}} = E_{\mathbf{k}}\, \varphi_{\mathbf{k}} = E_{\mathbf{k}}\, u_{\mathbf{k}}\, e^{i\mathbf{kr}}. \tag{12a}$$

The eigenvalues $E_{\mathbf{k}}$ differ from those of the operator H of (12) in first approximation by an amount of $-eF \int_\Omega u_{\mathbf{k}}^*\, x u_{\mathbf{k}}\, \mathrm{d}\tau$. The integration extends over the crystal volume Ω, over which the wave function is normalized. The time-dependent Schroedinger equation for the total Hamiltonian reads, after multiplication with $\varphi_{\mathbf{k}}^*$ and integration over the volume of the crystal:

$$a_{\mathbf{k}}\, E_{\mathbf{k}} - eF\, \Sigma_{\mathbf{k}'}\, a_{\mathbf{k}'}\, \Sigma_l\, x_l\, e^{i(k_{x'} - k_x)x_l} \int_{cell} e^{i(k_{x'} - k_x)x}\, u_{\mathbf{k}}^*\, u_{\mathbf{k}'}\, \mathrm{d}\tau = i\hbar\, \dot{a}_{\mathbf{k}}.$$

Transitions to other bands are neglected. The integral extends over the atomic cell at $x_l = 0$. For a very large crystal the term with the summation over l approaches $-iN(\partial/\partial k_x')\, \delta_{k_{x'}k_x}$, where N is the number of atoms in the crystal. Replacing the sum over $\mathbf{k}'$ by an integral, so that the Kronecker symbol becomes a δ function, and integrating by parts, we obtain

$$\hbar\, \partial a_{\mathbf{k}}/\partial t + eF\, \partial a_{\mathbf{k}}/\partial k_x + i a_{\mathbf{k}}\, E_{\mathbf{k}}^p = 0 \tag{15}$$

with

$$E_{\mathbf{k}}^p = E_{\mathbf{k}} - eF\, \xi_{\mathbf{k}}, \tag{15a}$$

where the real distance $\xi_{\mathbf{k}}$ is given by

$$\xi_{\mathbf{k}} = i \int_\Omega u_{\mathbf{k}}^* (\partial u_{\mathbf{k}}/\partial k_x)\, \mathrm{d}\tau - \int_\Omega u_{\mathbf{k}}^*\, x u_{\mathbf{k}}\, \mathrm{d}\tau. \tag{16}$$

These two integrals in (16) are for non-polar crystals only finite due to the spin-orbit interaction [24]). Both integrals measure the polarization for the state $\mathbf{k}$ in the x direction, the first for a wave packet, as we shall see below, and the second for the pure Bloch state. The energy $E_{\mathbf{k}}^p$ in (15) therefore represents the total energy connected with the wave function with wave vector $\mathbf{k}$

in the wave packet, and is independent of the actual shape of the packet. The mean value of a coordinate x_i of a wave packet

$$\langle x_i(t)\rangle = \Sigma_{\mathbf{k}} \Sigma_{\mathbf{k}'} \int_\Omega a_{\mathbf{k}}^* \varphi_{\mathbf{k}}^* x_i a_{\mathbf{k}'} \varphi_{\mathbf{k}'} \, d\tau$$

is found to be, when using the same procedure as for the evaluation of the Schroedinger equation

$$\langle x_i(t)\rangle = \Sigma_{\mathbf{k}} i a_{\mathbf{k}}^* \partial a_{\mathbf{k}}/\partial k_i + |a_{\mathbf{k}}|^2 q_i(\mathbf{k}) \tag{17}$$

where q_i is the i component of the polarization in the wave packet belonging to the state $\mathbf{k}$:

$$q_i(\mathbf{k}) = i \int_\Omega u_{\mathbf{k}}^* (\partial u_{\mathbf{k}}/\partial k_i) \, d\tau, \tag{18}$$

which is just the first part of $\xi_{\mathbf{k}}$ in (16). It manifests itself therefore as a property of a pure Bloch state, though it exists only when a wave packet is formed. For the pure Bloch state the last term of (16) is found for q_x. A similar difference is thus found in the energies $E_{\mathbf{k}}^p$ and $E_{\mathbf{k}}$. This existence of two forms for the energy necessitates this more rigourous analysis, since it is for instance not certain *a priori* that both E's occurring in (11) are identical.

The velocity in the y direction of the wave packet is found by differentiating (17) with respect to t and using (15), and is given by

$$\langle v_y\rangle = \Sigma_{\mathbf{k}} |a_{\mathbf{k}}|^2 \hbar^{-1} (\partial E_{\mathbf{k}}^p/\partial k_y) + (\partial |a_{\mathbf{k}}|^2/\partial t) \, q_y(\mathbf{k}), \tag{19}$$

since a term containing $F(\partial/\partial k_x)$ is zero.

For the expectation value of H_T for the wave packet is found

$$\langle E\rangle = \Sigma_{\mathbf{k}} |a_{\mathbf{k}}|^2 E_{\mathbf{k}}^p - ieF a_{\mathbf{k}}^* \partial a_{\mathbf{k}}/\partial k_x. \tag{20}$$

The equations (19) and (20) have the form as if an electron in a pure Bloch state has a velocity $\hbar^{-1} V_{\mathbf{k}} E_{\mathbf{k}}^p$ and an energy $E_{\mathbf{k}}^p$. In the absence of skew scattering (see below) no driving force in the y direction is present. Thus, apart from the shift of the Fermi sphere into the x direction, the density function $\varrho_{\mathbf{k}} = \overline{|a_{\mathbf{k}}|^2}$ is then the Fermi-Dirac function of this $E_{\mathbf{k}}^p$, so that (11) applies.

The last term of (19) represents the polarization current which has been discussed above, and can give only a contribution if in the mean $\partial |a_{\mathbf{k}}|^2/\partial t \neq 0$.

The only possibility for getting a finite spontaneous Hall effect is that ϱ in (11) has not the value corresponding to thermal equilibrium, but that the Fermi "sphere" is shifted not only into the x direction, but also into the y direction. This has to be caused by the collision processes, which have not yet been considered. The spin-orbit interaction has therefore to make the scattering skew, *i.e.* for an incident electron moving in the x direction the amplitude of the outgoing wave has to be different for opposite values of k_y of this scattered wave. We shall investigate this problem in the following sections.

11. The effect of spin-orbit interaction on the transition probability

In order to proceed with the discussion of effects which do not yield a finite spontaneous Hall effect in ferromagnetic materials, we shall treat the electron scattering process in the usual way, *i.e.* by using transition probabilities, and we shall show that under that condition the spin-orbit interaction does not give skew scattering. For this purpose we shall first discuss some properties of the Bloch functions. A Bloch function can be expanded into its Fourier components as follows:

$$\varphi_{\mathbf{k}}(\mathbf{r}) = e^{i\mathbf{k}\mathbf{r}} \Sigma_{\mathbf{g}} A_{\mathbf{g},\mathbf{k}} e^{i\mathbf{g}\mathbf{r}}, \tag{21}$$

where $\mathbf{g}$ is a vector of the reciprocal lattice. Since we have to do with non-polar crystals, the Hamiltonian is invariant under a transformation of $\mathbf{r} \rightarrow -\mathbf{r}$. Therefore when (21) undergoes the same transformation, it must remain a solution for the same value of the energy. If there is no spin-orbit interaction the Schroedinger equation is a differential equation with real coefficients, and therefore the complex conjugate (c.c.) of (21) is also a solution of it for the same value of the energy. Combining these two facts, it follows that we can take all $A_{\mathbf{g},\mathbf{k}}$'s as real. If the spin-orbit interaction (9) is included, this is no longer true because of the occurrence of a term linear in $\mathbf{p}$. It is seen by perturbation calculus that the extra terms in $A_{\mathbf{g}}$ linear in the spin magnetic moment $\boldsymbol{\mu}$ have a purely imaginary coefficient. This is also clear from the fact that taking the c.c. of the Hamiltonian (reversal of time) is the same as reversing the spin direction, from which follows

$$A_{\mathbf{g},\mathbf{k}}(\boldsymbol{\mu}) = A^*_{-\mathbf{g},-\mathbf{k}}(-\boldsymbol{\mu}).$$

Since the Hamiltonian is still invariant against the transformation $\mathbf{r} \rightarrow -\mathbf{r}$, we have

$$A_{\mathbf{g},\mathbf{k}}(\boldsymbol{\mu}) = A^*_{\mathbf{g},\mathbf{k}}(-\boldsymbol{\mu}).$$

We shall now calculate the transition probability of an electron from the state $\mathbf{k}$ to the state $\mathbf{k}'$ under the action of a perturbing potential V, which includes the spin-orbit interaction accompanying it. This transition probability is proportional to

$$P_{\mathbf{k}\mathbf{k}'} \sim |\langle \mathbf{k}'|V|\mathbf{k}\rangle|^2 \tag{22}$$

and enters into the Boltzmann integral equation, from which the stationary change in the distribution function under the action of an applied electric field can be calculated. For free electrons this procedure is equivalent to the Born approximation. We shall show that $P_{\mathbf{k}\mathbf{k}'}$ does not contain terms linear in $\boldsymbol{\mu}$, and therefore we cannot obtain a spontaneous Hall effect in this approximation. If we take into account the effect of spin-orbit interaction in φ, we can leave it out in V and *vice versa*.

Starting with the first case, and expanding this V into a Fourier series

$$V = \Sigma_{\mathbf{q}} V_{\mathbf{q}} e^{i\mathbf{q}\mathbf{r}}, \tag{23a}$$

where $\mathbf{q}$ can be any vector, we obtain

$$\langle \mathbf{k}'|V|\mathbf{k}\rangle = \Sigma_{\mathbf{g}} \Sigma_{\mathbf{g}'} V_{(\mathbf{k}'-\mathbf{k}+\mathbf{g}'-\mathbf{g})} A_{\mathbf{g},\mathbf{k}} A^*_{\mathbf{g}'\mathbf{k}'}. \tag{24a}$$

By squaring the absolute value of this expression, we get products such as $V_{\mathbf{q}_1} V^*_{\mathbf{q}_2}$. We assume a random perturbing potential so that the phases of the $V_{\mathbf{q}}$'s are uncorrelated. This means that the mean value of the product is only finite if $\mathbf{q}_1 = \mathbf{q}_2$. We then get for the transition probability, being a real number, a sum of terms of the fourth degree in the $A_{\mathbf{g}\,\mathbf{k}}$'s with real coefficients. Therefore it cannot contain a term linear in $\boldsymbol{\mu}$, which can only be imaginary.

The next step is to take into account the extra spin-orbit interaction due to the perturbing potential, so that now the $A_{\mathbf{g},\mathbf{k}}$'s can be taken as real. The Fourier expansion now becomes, according to (9) and (23*a*):

$$V' = \Sigma_{\mathbf{q}} V_{\mathbf{q}} e^{i\mathbf{q}\mathbf{r}} [1 + i(2mec)^{-1} (\boldsymbol{\mu} \times \mathbf{q})\, \mathbf{p}]. \tag{23b}$$

Instead of (24*a*) we now obtain

$$\langle \mathbf{k}'|V'|\mathbf{k}\rangle = \Sigma_{\mathbf{g}} \Sigma_{\mathbf{g}'} V_{(\mathbf{k}'-\mathbf{k}+\mathbf{g}'-\mathbf{g})} \times [1 + i\,\hbar\,(2mec)^{-1} \{\boldsymbol{\mu} \times (\mathbf{k}' - \mathbf{k} + \mathbf{g}' - \mathbf{g})\}\, (\mathbf{g} + \mathbf{k})]\, A_{\mathbf{g}\mathbf{k}}\, A_{\mathbf{g}'\mathbf{k}'}. \tag{24b}$$

Also in this case, due to the assumption of random phases of $V_{\mathbf{q}}$, the only imaginary numbers occurring in the expression for $P_{\mathbf{k}\mathbf{k}'}$ are those in the terms with $\boldsymbol{\mu}$. Since $P_{\mathbf{k}\mathbf{k}'}$ is real, $\boldsymbol{\mu}$ can only occur with even powers. The conclusion is therefore that the Born approximation of the scattering process cannot yield a finite spontaneous Hall effect.

We shall illustrate the assumption of random phases of the Fourier components of (23*a*) with some simple examples. Firstly, it is clear that it applies to lattice vibration scattering, where the phases of the lattice waves are not defined. Secondly, for one single symmetrical potential trough at the origin all $V_{\mathbf{q}}$'s are real. In that case $V_{\mathbf{q}_1} V_{\mathbf{q}_2}$ is not zero for $\mathbf{q}_1 \neq \mathbf{q}_2$, but our conclusion remains valid. For a number of identical potential troughs distributed at random over the lattice, the Fourier coefficients $V_{\mathbf{q}}$ of (23*a*) change into $V_{\mathbf{q}} \Sigma_n e^{i\mathbf{q}\mathbf{a}_n}$ if the troughs are centred around $\mathbf{a}_n$. For the transition probability we then get terms which contain the products

$$V_{\mathbf{q}_1} V_{\mathbf{q}_2} \Sigma_n \Sigma_m e^{i(\mathbf{q}_1\mathbf{a}_n - \mathbf{q}_2\mathbf{a}_m)}.$$

For the random distribution it is clear that only the terms for which $\mathbf{q}_1 = \mathbf{q}_2$ and $m = n$ contribute, which agrees with our assumption.

In the approximation used above the scattering is proportional to V^2. If it had given a finite result for the spin-orbit interaction scattering, we should have found $R_s \sim \varrho$. The next terms contain V^3 or V^4, so that we must expect that R_s varies at least as $\varrho^{3/2}$ or ϱ^2. Such a dependence on ϱ is actually observed.

12. Non-central collisions due to spin-orbit interaction

Since we have shown that the Born approximation does not yield a spontaneous Hall effect, we have to treat the scattering problem more rigourously.

The idea is that in the periodic lattice the transverse spin-orbit force is compensated by "electrostatic" forces for a finite value of the polarization. At the place of a perturbation, *e.g.* due to a foreign atom, this equilibrium situation is destroyed, and a transverse force results, which accelerates the electron in that direction. Two models are discussed which stress the changes due to the perturbation of the spin-orbit force and of the "electrostatic" forces respectively.

a. Non-spherical perturbing potential

As an example we shall treat the scattering of free electrons on a rectangular potential with radius R with a value for $r < R$:

$$V = (h^2/2m)\,(k^2 - k_1^2) \tag{25}$$

and $V = 0$ for $r > R$, where $\mathbf{k}$ is the wave vector of the incident wave in the x direction. Using spherical coordinates, defined by $x = r\cos\vartheta$, $-z + iy = r\sin\vartheta\, e^{i\varphi}$, the solution of the problem without spin-orbit interaction is given by

$$r < R:\quad \psi = \Sigma_l\, a_l j_l(k_1 r)\, P_l(\cos\vartheta)$$
$$r > R:\quad \psi = \Sigma_l\,(2l+1)\, i^l\, j_l(kr)\, P_l(\cos\vartheta) + b_l h_l(kr)\, P_l(\cos\vartheta);$$

here $j_l(\varrho) = (\pi/2\varrho)^{\frac{1}{2}}\, J_{l+\frac{1}{2}}(\varrho)$ is the spherical Bessel function, $J_{l+\frac{1}{2}}$ being the ordinary Bessel function of half-odd-integer order. Further $h_l = j_l + in_l$, where n_l is in a similar way the spherical Neumann function so that h_l is a spherical Hankel function (cf. Schiff[25]). At $r = R$ the two solutions must have equal values of the function and its first derivative, these conditions being sufficient for solving a_l and b_l. If the Hamiltonian of this problem is denoted by H and the wave function by ψ, then introduction of the spin-orbit operator H' of (9) with $\boldsymbol{\mu}$ along the z-axis gives a change in the wave function of ψ', so that in first approximation

$$(H - E)\,\psi' = -H'\,\psi.$$

In spherical coordinates the operator H' of (9) is given by

$$H' = i\,(h/2mc)^2\,(M_z/M)\,(r^{-1}\,\partial V/\partial r)\sin\varphi\,\partial/\partial\vartheta, \tag{9c}$$

where M_z and M are the z component and the absolute value of the magnetization respectively. In our case this operator is zero everywhere apart from $r = R$. The wave function ψ' is given by

$$r < R:\quad \psi' = \Sigma_l\, p_l j_l(k_1 r)\sin\varphi\,\partial P_l(\cos\vartheta)/\partial\vartheta$$
$$r > R:\quad \psi' = \Sigma_l\, q_l h_l(kr)\sin\varphi\,\partial P_l(\cos\vartheta)/\partial\vartheta.$$

At $r = R$ we must have

$$p_l j_l(\alpha) - q_l h_l(\beta) = 0$$
$$p_l \alpha j_l'(\alpha) - q_l \beta\, h_l'(\beta) = -\, i(\hbar/2mc)^2\, (M_z/M)\, (k_1^2 - k^2)\, a_l,$$

where $\alpha = k_1 R$ and $\beta = kR$. If α and β are small we obtain for the scattering cross section for the resistivity in first approximation

$$A_x \sim |b_0|^2 \qquad A_y \sim (i/\sqrt{3})\, (b_0^* q_1 - b_0 q_1^*).$$

The Hall angle is defined as

$$\varphi_{SH} = -\, A_y/A_x. \tag{26}$$

For small values of α and β the result can be found by series expansion, and one obtains in first approximation

$$\varphi_{SH} = -\, (2/3\sqrt{3})\, (\hbar/2mcR)^2\, (M_z/M)\, (\alpha^2 - \beta^2)\, \beta^3. \tag{26a}$$

Since $(\alpha^2 - \beta^2)$ is proportional to V, the result is that $R_s \sim \varrho^{3/2}$. Another consequence is that φ_{SH} has opposite sign for attractive and repulsive perturbing potentials. For a repulsive potential it is positive. The order of magnitude is, however, far too small to account for the experimental values. For instance for $\beta = 1$, $|\alpha^2 - \beta^2| \approx 1$ and $R = 10^{-8}$ cm we find $\varphi_{SH} = 1.4 \times 10^{-6}$, as compared with 10^{-2} for the observed values.

b. Non-central collision

So far we have only considered the influence of spin-orbit interaction on the perturbing potential. We have seen, however, that spin-orbit interaction severely modifies the Bloch wave functions, in so far that it gives them a polarization **q** in a direction perpendicular to both the velocity and the spin. If, as in a disordered alloy, one of the atoms is replaced by a foreign one, the electrons will not collide centrally on this perturbing potential. As a result one can expect a transverse current, which is here a Hall current. We shall illustrate this with the simplest model of a spherically symmetrical potential function. For the incident wave we take only one term of the actual wave function, *i.e.*

$$\psi = e^{ik_x x} \cos(g_y y - \gamma) = \tfrac{1}{2}\, [e^{-i\gamma}\, e^{i(k_x x + g_y y)} + e^{i\gamma}\, e^{i(k_x x - g_y y)}]. \tag{27}$$

This wave function is modulated in the y direction with the periodicity of the lattice (g_y is the shortest reciprocal lattice vector). The phase angle is related to the polarization or impact parameter q_y of (18) by

$$\gamma = g_y q_y. \tag{28}$$

The two waves into which ψ can be resolved have total wave vectors of equal magnitude

$$k = (k_x^2 + g_y^2)^{\frac{1}{2}} \tag{29}$$

and have directions lying in the $y-z$ plane which make angles $\pm\,\varepsilon$ with the x axis satisfying

$$\tan\varepsilon = g_y/k_x. \tag{30}$$

The scattering of these two waves can be calculated separately. The asymptotic form of the scattered wave of an incident wave $e^{i\mathbf{kr}}$ is [26])

$$\psi_s \approx r^{-1}\, e^{ikr}\, f(\vartheta) = (e^{ikr}/2ikr)\, \Sigma_{l=0}^{\infty}\, (2l+1)\, (e^{2i\eta_l}-1)\, P_l\,(\cos\vartheta), \tag{31}$$

where ϑ refers to the direction of $\mathbf{k}$. The two waves (27) have in (31) all factors common, except the last where ϑ refers to two different orientations. The total scattered wave is therefore in this case

$$\psi_s \approx (e^{ikr}/2ikr)\, \Sigma_{l=0}^{\infty}\, (2l+1)\, (e^{2i\eta_l}-1)\, [\tfrac{1}{2}e^{-i\gamma}\, P_l\,(\cos\vartheta_1) + \tfrac{1}{2}e^{i\gamma}\, P_l\,(\cos\vartheta_2)], \tag{31a}$$

where ϑ_1 and ϑ_2 satisfy

$$\cos\vartheta_{1,2} = \cos\vartheta\,\cos\varepsilon \pm \sin\vartheta\,\sin\varepsilon\,\sin\varphi.$$

For small perturbing potentials the spontaneous Hall angle (26) is found to be

$$\varphi_{SH} = -\frac{A_y}{A_x} = \frac{8\sqrt{3}\,\sin\gamma\,\cos\gamma\,\sin\varepsilon\,\sin\eta_0\,\sin(\eta_0-\eta_1)\,\sin\eta_1}{16\,\sin^2\eta_0\,\cos^2\eta_0\,\cos^2\gamma} \approx \tfrac{1}{2}\sqrt{3}\,\gamma\eta_1, \tag{32}$$

since for small k_x, according to (30), $\varepsilon \approx \pi/2$. It has opposite sign for repulsive and attractive potentials, as one would expect. For our rectangular potential function we can calculate η_1 and find for small R:

$$\eta_1 = (\alpha^2 - \beta_g^2)\, \beta_g^3\, /45,$$

where $\beta_g = g_y R$, so that

$$\varphi_{SH} \approx (\sqrt{3}/90)\, \gamma(\alpha^2 - \beta_g^2)\, \beta_g^3. \tag{32a}$$

This formula is quite similar to (26*a*), in both cases $R_s \sim \varrho^{3/2}$. This similarity is due to the fact that in both cases we have to do with non-central collision. In the first case the impact parameter follows from (9*b*) and is equal to

$$q_y' = v_x\mu_z/2ec = \tfrac{1}{2}(v_x/c)\, (\hbar/2mc), \tag{33}$$

which is very small (3×10^{-14} cm for $v_x = 10^8$ cm/sec). It corresponds to a negative γ in (32*a*), and therefore the signs of (32*a*) and (26*a*) are the same for the same potential. The value of q_y of (18) and (28) is much larger. It can be deduced from the K–L paper that it is of the order of 10^{-9} cm. This means that the translational velocity gives rise to an orbital angular momentum which is of the same order of magnitude as that which follows from the g factor [27]), being equal to $(g-2)\hbar/2$. The estimation of K–L is very rough, for instance in their eq. (4.2) a spin-orbit field of the type (9*a*) is introduced where it had to be one of the type

$$\mathbf{H}'_{s.o.} = \mathrm{curl}\,(\boldsymbol{\mu}\times\mathbf{E})/2e \tag{9c}$$

(compare (9)). But in view of the interpretation in terms of the orbital angular momentum, the estimation seems reasonable, though it would then have been possible to estimate q_y on this base at once. For $q_y = 10^{-9}$ cm, one finds from (28) $\gamma \approx 0.2$. For a reasonable value of η_1, say 0.1, we find $\varphi_{SH} \approx 0.02$, this being of the correct order of magnitude.

D. Polder has kindly pointed out to the author that it would be better to attack the second problem (model *b*) with the effective mass theory. The application of this theory allows one to insert directly the enlarged q_y into (9*c*), so that the result also becomes of the right order of magnitude. Unfortunately this theory is only applicable for smoothly varying potentials, *i.e.* to those which are spread out over several atoms, and which are small as compared with the energy differences between the relevant bands. Neither of these conditions is fulfilled for the perturbing potentials in metals. For instance the potentials due to foreign atoms, in which we are particularly interested, can be represented by a screened Coulomb potential

$$V = (Ze^2/r)\, e^{-r/r_0}$$

with r_0 of the order of 0.3×10^{-8} cm, which value has also to be considered as the radius of the effective potential. The effective depth for $Z = 1$ is of the order of 50 eV, which value is much larger than the mean energy separation of different bands. For semi-conducting ferromagnetics, as for instance the ferrites, this effective mass theory undoubtedly gives the most adequate description. It may be noted that also in ferrites a spontaneous Hall effect has been observed [28]).

The model *b*, analyzed above, has therefore at least the merit that it holds to some approximation in the situation which occurs in metals, (e.g. (32) is only valid for R smaller than the lattice parameter) though it may be doubted whether the wave function used has the adequate features.

So far we have not yet discussed the type of wave functions of the electrons involved. The effective electrons must have a net magnetization, which condition is satisfied for the 3*d* electrons. Usually, however, one assumes that the main part of the current is carried by the 4*s*-*p* electrons. We have seen in chapter I, however, that, in order to explain several properties of transition metals, one has to adopt Bloch functions for the 3*d* electrons, *i.e.* they are assumed to wander through the crystal, and to be able to carry a current. If we assume that these 3*d* electrons give the spontaneous Hall effect, we have still to multiply the φ_{SH} of (32) with the square of the ratio of the conductivity of the *d* electrons and the total conductivity.

A second possibility is, however, that the *s* electrons, even if they are not magnetized, give the spontaneous Hall effect, since, as we shall see in the next chapter, at temperatures well below the Curie temperature most of the current is carried by the *s* electrons having their spin parallel to the net magnetization. It is also shown in that chapter, however, that this is probably

not the case for the alloys with non-magnetic elements at low temperatures. Since the latter have extremely high values of R_s, we can rule out this possibility on experimental grounds.

One essential feature of the models used was, that in first approximation the spontaneous Hall effect should have opposite sign for repulsive and attractive potentials. With this in mind we had measured Ni alloys with elements which have lower and higher atomic numbers respectively than that of nickel, for instance Al or Si at one side and Sn or W on the other. For all these alloys, however, φ_{SH} is negative. One might think that, since these foreign atoms do not have d orbits available with comparable energy, these ions always act as a kind of repulsive potential for the $3d$ electrons. For $\gamma > 0$ in (32) one then finds $\varphi_{SH} < 0$. Such a reasoning cannot be given, however, for the Ni-Co as compared with the Ni-Cu alloys. In chapter III we shall give strong evidence that the Cu ions are magnetized, so that we have to expect that φ_{SH} has opposite sign for these alloys, which is not the case.

For lattice vibration scattering the mean value of the perturbing potential is zero, so one cannot expect a result odd in V. The adequate theory of the scattering of Bloch waves on phonons in the presence of spin-orbit interaction must therefore give in first approximation $\varphi_{SH} \sim V^2$. Thus especially for pure metals should hold $R_s \sim \varrho^2$, as in the $K - L$ theory. This was found to be approximately true for iron [24]).

In order to treat this case, we have worked out the series expansion concerning mechanism a one step further and found, for the case that V averages to zero, the mean spontaneous Hall angle to be

$$\bar{\varphi}_{SH} = -\bar{A}_y/\bar{A}_x = -(28/45\sqrt{3})(\hbar/2mcR)^2 (M_z/M) \overline{(\alpha^2 - \beta^2)^2}\,\beta^3 \quad (26b)$$

This result is practically equal to (26a), only $(\alpha^2 - \beta^2)$ is replaced by its mean square. For the same assumptions the value of (26b) will be -1.3×10^{-6}. It appears that terms with still higher powers of $(\alpha^2 - \beta^2)$ have substantially smaller coefficients.

When using this result in the effective mass approximation, we have again to multiply (26b) with the ratio of q_y of (18) and q'_y of (33), being of the order of 3×10^4, yielding $\varphi_{SH} = -0.04$, which is of the right order of magnitude, and independent of the sign of V. Thus $\varphi_{SH} \sim \varrho$ or $R_s \sim \varrho^2$.

Of course the approximations made are invalid, but the results obtained may indicate that the V^2 terms in φ_{SH} are at least comparable to the V terms.

CHAPTER III

THE MAGNETORESISTANCE OF FERROMAGNETIC METALS AND ALLOYS

13. Introduction

It is well known [29]) that in strong magnetic fields the resistivity at finite temperatures of ferromagnetic metals varies about linearly with the field, the small negative slope being the same for all orientations (fig. 8). As in

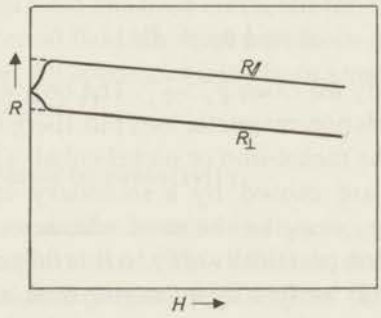

Fig. 8. Schematical plot of the longitudinal and transversal resistances for ferromagnetic metals.

chapter II we are only interested in the effects at saturation and the straight lines are extrapolated to $H = 0$. Whether this has to be $B = 0$ as in ch. II, or $H = 0$, is of minor importance here. It appears that this resistivity is anisotropic for a fixed orientation of the magnetization. The elements of the resistivity tensor with respect to the cubic axes can then, for reasons of symmetry, be written as

$$\begin{aligned} \varrho_{11} &= \varrho_0 + \varrho_1 \alpha_1^2 + \varrho_3 (\alpha_2^2 \alpha_3^2 + \alpha_3^2 \alpha_1^2 + \alpha_1^2 \alpha_2^2) + \varrho_5 \alpha_2^2 \alpha_3^2 \\ \varrho_{12} &= \varrho_2 \alpha_1 \alpha_2 + \varrho_4 \alpha_1 \alpha_2 \alpha_3^2. \end{aligned} \tag{1}$$

Terms higher than those of the fourth degree in the direction cosines α_i of the magnetization with respect to the crystal axes being omitted. Similar equations are holding for the other tensor elements.

For nickel and iron all five constants of (1) have been determined [30]) at room temperature.

If we confine ourselves to the quadratic terms, we find for the resistivity

in an arbitrary orientation characterized by the direction cosines β_1, β_2 and β_3:

$$\varrho = \varrho_0 + \varrho_1(\alpha_1\beta_1 + \alpha_2\beta_2 + \alpha_3\beta_3)^2 + 2(\varrho_2 - \varrho_1)(\alpha_2\alpha_3\beta_2\beta_3 + \\ + \alpha_3\alpha_1\beta_3\beta_1 + \alpha_1\alpha_2\beta_1\beta_2) \ldots . \quad (2)$$

Here $\varrho_1 = \varrho_{/\!/} - \varrho_\perp$ if the magnetization is along the cubic axis, and ϱ_2 that if it is along the body diagonals. The effect is isotropic if $\varrho_1 = \varrho_2$, the resistivity then only depends upon the angle between the magnetization and the current; the material then has uniaxial properties with the magnetization vector as axis of symmetry. For a polycrystalline material with at random orientation of the crystals we observe the same symmetry. The resistivity can then also be described with the equation

$$\varrho(\theta) = \varrho_{/\!/} \cos^2\theta + \varrho_\perp \sin^2\theta, \quad (3)$$

θ being the angle between the electrical current and the magnetic field. In the demagnetized state usually

$$\varrho = \tfrac{1}{3}\varrho_{/\!/} + \tfrac{2}{3}\varrho_\perp. \quad (4)$$

It appears that in nearly all cases $\varrho_{/\!/} > \varrho_\perp$. The only exceptions found so far occur in some alloys with non-magnetic ions but there the effect is a hundred times smaller than in the nickel-iron or nickel-cobalt alloys. It will be shown that these exceptions are caused by a secondary effect. We regard this positive sign of $\Delta\varrho = \varrho_{/\!/} - \varrho_\perp$ as the most characteristic feature, and we shall confine our attention practically only to this first order effect. Expressed in the constants of eq. (2) we find by averaging over all orientations:

$$\varrho_{/\!/} - \varrho_\perp = \tfrac{2}{5}\varrho_1 + \tfrac{3}{5}\varrho_2. \quad (5)$$

Since the anisotropy is not large (at most 20%), the way of averaging (for instance over the conductivity or over the resistivity) is of minor importance, as is symbolized by the approximate equality of $(1 - x)^{-1}$ and $(1 + x)$ for $x \ll 1$.

The finite negative slope of the ϱ-H curve is connected with the increase of the intrinsic magnetization in strong fields against the action of the temperature agitation, by which the saturation moment is decreased. One should expect this effect to be zero at $T = 0$. This is satisfied for most alloys, but we shall see that there do occur some exceptions.

The phenomenological description of these effects is the same as for the magnetostriction. The anisotropy of the resistivity is analogous to the linear magnetostriction (anisotropy of the dimensions) both being a tensor quantity in dependence of the orientation of the magnetization vector. The decrease of ϱ in strong fields corresponds to the volume magnetostriction. The magnetostriction itself should also change the resistance of the sample, but these variations are far too small to explain the experimental values.

At low temperatures in the pure metals we still encounter a third type of change in resistivity with the field, which is superimposed on the foregoing ones. It is the normal increase in resistivity which we also have in non-ferromagnetic metals. It is somewhat different because we shall show that we have to take here as effective field that which is used to describe the Hall effect, as is discussed in ch. II, instead of the applied field H, as is always sufficient in the non-ferromagnetic metals. We shall discuss the different types of magnetoresistance separately.

14. Experimental technique

The measurements have been performed in the large magnet of the Kamerlingh Onnes Laboratory, the maximum fieldstrength used being about 22000 oersteds. The resistances have been measured in the usual way on a potentiometer as in chapter II. For most measurements wires have been used, with a length of about 25 mm and a diameter of some tenths of a mm. In this case the transversal external field has been corrected for the demagnetizing field in order to find the internal field. In some cases foils of some tenths of a mm thicknes were available. All specimens have been annealed in purified hydrogen as described in chapter II.

15. The normal increase in resistivity

At low temperatures a similar increase in the resistance has been found as for the non-ferromagnetic metals. This effect is due to the Lorentz force acting on the conduction electrons, which gives them curved paths. The effect is appreciable only if the mean free path is comparable with the radius of curvature, which is inversely proportional to the field strength. Accordingly for the alloys the effect was small.

For the pure metals Ni and Fe at liquid hydrogen temperatures the effects are large and of the same order of magnitude as for the noble metals. Here $\varrho_\perp$ always exceeds $\varrho_{/\!/}$.

The main difference between the curves for the ferromagnetic metals and those for the normal ones was that for Ni and Fe at weak fields the difference between longitudinal and transversal resistance did not vanish, except of course for $H = 0$, since the remanence of the material is negligible (fig. 9). The only possible conclusion is that the field acting on the conduction electrons is not equal to the external field, but a field caused by the internal dipoles has to be added. In the case of iron we were able to evaluate this extra field by means of the Kohler diagram. K o h l e r [31]) has stated that $\Delta\varrho/\varrho_{H=0}$ can be plotted as a function of $H/\varrho_{H=0}$ only, for all temperatures and purities. The diagram in which log $(\Delta\varrho/\varrho)_{H=0}$ is plotted *versus* log $(H/\varrho_{H=0})$ is called the "Kohler diagram". The values of the additive internal field and those of $\varrho_{H=0}$ (which define an additive constant in $\Delta\varrho_{/\!/}$ and $\Delta\varrho_\perp$)

can now be chosen in such a way as to fit all the points on a Kohler diagram. The actual procedure for doing this was as follows.

Firstly we have to correct for the orientation effect described by (3). For iron this amounted to 0.5% at room temperature, and we assumed this to be independent of the temperature, as was found approximately for nickel (see section 17). Because of the smallness of this effect for iron no large error can be introduced. The values of the resistance at zero total field could be extrapolated with sufficient accuracy. By plotting the Kohler diagram with different values for the additive internal field, and taking for $\Delta\varrho$ the difference

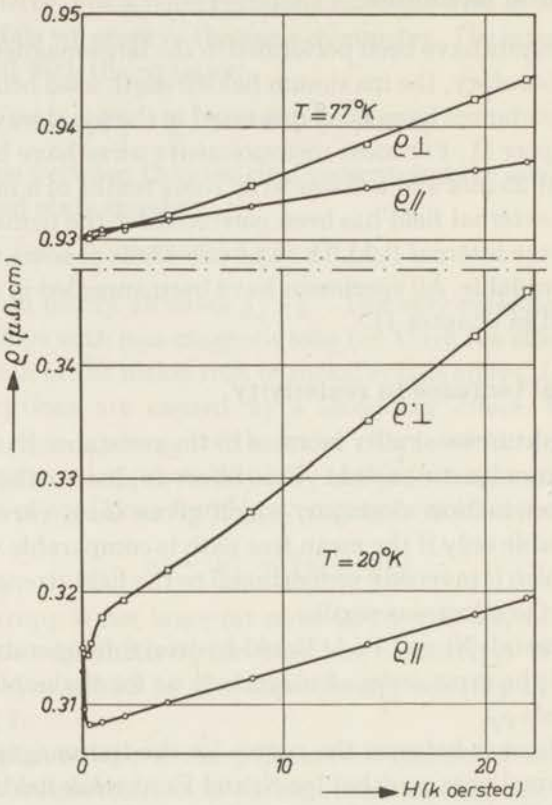

Fig. 9. Magnetoresistance of iron at low temperatures.

between $\varrho_\perp$ and $\varrho_{/\!/}$, we found that all measurements (at $T = 14$, 20, 64, 69 and 77°K), especially for the purest specimen, lie on one straight line for an extra field of 22000 $\pm$ 1000 oersted. This is approximately equal to $4\pi M$. Thus the field acting on the conduction electrons is equal to the induction **B**, which is the mean magnetic field within the metal. Now the curves for $\Delta\varrho_\perp/\varrho$ and $\Delta\varrho_{/\!/}/\varrho$ could be derived separately (fig. 11). Three specimens have been used of different purity (labelled from I to III in fig. 10, I being the most impure one and III the purest). In order to avoid crowding not all

experimental points are given in the figure. It is seen that the three curves do not coincide, and that the curve for the most impure metal is highest.

For nickel the extra internal field could not be estimated with the same accuracy as for iron, and may range from 6 to 12 k oersted. The reasons may be firstly that in the Kohler diagram no straight lines were obtained and secondly that the ferromagnetic orientation effect is much greater (3%). Therefore we took for the additive field also $4\pi M$ (6000 gauss). The results are given in fig. 11. From this figure we see that the transversal effect in iron shows no saturation, whereas nickel behaves similarly to the odd-valent metals, with the exception that the ratio between the longitudinal and the transversal effect increases with increasing field or decreasing temperature.

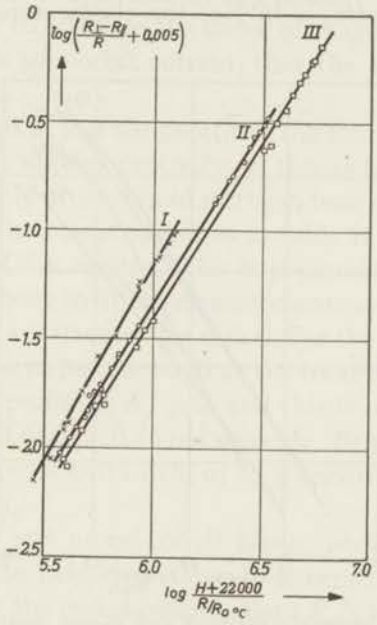

Fig. 10. Reduced Kohler diagram for iron. For ΔR the difference between $R_{\parallel}$ and $R_{\perp}$, corrected for the orientation effect (1), has been taken. The three specimens have different purity (I is the impurest, and III the purest one). The lower points refer to measurements at temperatures of liquid nitrogen, and the higher ones to temperatures of liquid hydrogen.

For comparison in the Kohler diagram we have also plotted the transversal curve for sodium, which is lower than those for iron and nickel.

The magnetoresistance in metals is caused by the fact that not all electrons have the same drift velocity. The effective Lorentz force, giving rise to the Hall effect, is then not the same for all electrons. If the Hall current is compensated by an externally applied electric field, which gives the same force on all electrons, not all curvatures are compensated, but some curvatures survive, though with a smaller value, and others are over-compensated. It is

seen then that the current in the x direction is decreased, *i.e.* the resistivity has increased. At finite temperatures there is already a spread in the magnitude of the velocities of the conducting electrons, and therefore in the drift velocities, but this is far too small to explain the experimental values. Very much greater spread is present if the Fermi surface in **k** space is not spherical, or if the intensity of scattering is anisotropic and depends on both the initial and the final state, and not only on the difference in velocity. The latter case occurs for lattice vibration scattering if the metal is elastically anisotropic. For sodium it is generally assumed that the Fermi surface is practically spherical. The observed magnetoresistance has therefore to be attributed to the anisotropic scattering. This is quite well possible since the elastic constants are very anisotropic in Na: the elastic anisotropy, expressed by

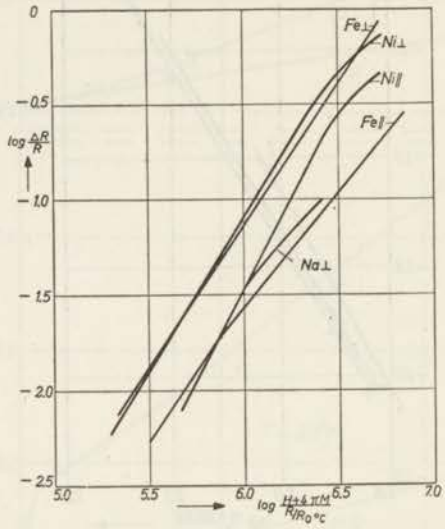

Fig. 11. Reduced Kohler diagrams for iron and nickel, both for the magnetic field parallel and perpendicular to the current. The transversal curve for sodium has been added for comparison.

the ratio $2c_{44}/(c_{11} - c_{12})$, is about 8. We assume, in agreement with our considerations of chapter I, that in nickel the s electrons carry the greater part of the current. If it is assumed that the magnetoresistance in Ni has the same origin as in Na, then one should expect that it is much smaller in the former, since this ratio of the elastic constants is only 2.6 in nickel. If there were no interaction with the $3d$ electrons, this would be the only possibility, since the s band is only occupied by 0.6 electrons per atom, so that the Fermi surface is far from any Brillouin zone boundary and will therefore be spherical. The high value of the magnetoresistance in nickel, and presumably also in iron, has therefore to be attributed to the non-

spherical Fermi surface as is plotted in fig. 4, which is caused by the mixing with $3d$ states.

The spontaneous Hall effect, as discussed in chapter II, also gives for moving electrons curved paths. Also these curvatures are different for different Bloch functions, so that a transverse field, which cancels out the resultant Hall current, will not do so all individual curvatures. In this respect the situation is the same as for the normal Hall effect, so that an increase in resistivity will also result. The spontaneous Hall effect could be described phenomenologically by introducing an extra effective magnetic field of magnitude $H_{eff}=(R_s/R_0)4\pi M$. Though it was realized that the action of spin-orbit forces is quite different from that of a homogeneous magnetic field, we shall assume, in order to estimate the order of magnitude of the change in resistivity due to this spin-orbit current, that the same field is active for the magnetoresistance.

For very pure metals at low temperatures the total effective field is therefore equal to **B**. This applies probably to the nickel and the purest iron, though it does not apply at the liquid nitrogen temperatures. For nickel, for instance, we find for the purest specimen in table II that at 77°K the extra field is of the order of 3 k oersted. This is presumably the reason that the procedure described above to fit the measurements at different temperatures on one curve was least satisfactory for nickel. For the purest iron specimen it is gratifying that we have just found **B** as the total effective field. Probably for the impurer iron specimens $R_s \neq 0$, and this is perhaps the reason that the curves I, II and III of fig. 10 do not coincide. Bringing I into coincidence with III should require an extra field of 15 k oersted at the lowest temperatures, *i.e.* $R_s \approx 0.7\ R_0$.

For the nickel-iron and nickel-cobalt alloys, according to table II, R_s is small, corresponding to fields less than 10 k oersted, so that its effect is hardly detectable. For the nickel-copper alloys R_s is larger, being equivalent to a field of 29k oersted for Ni82Cu18 at 20°K. If we use this field tentatively in fig. 10 and take for the resistivity at 0°C that of nickel or iron, we find for $\Delta\varrho/\varrho \approx -6\times 10^{-5}$, which is again too small to be significant. Actually it will be still smaller, since the effective field presumably only acts on the $3d$ electrons.

For the alloys with non-magnetic elements, however, the effective fields are much larger. For the Mo alloy, for instance, it is 350 k oersted at $T = 20°K$. We then find from fig. 10 $\Delta\varrho/\varrho \approx -2\times 10^{-3}$. Van Elst and Gorter[32]) have measured the magnetoresistance of several nickel alloys, and found them to be negative ($\varrho_{/\!/} < \varrho_{\perp}$) in Ni92Mo8 and Ni99Cr1 (weight %) having at 14°K the values -0.7×10^{-3} and -1.6×10^{-3}. For the Mo alloy, of which we have measured the Hall effect, $\Delta\varrho/\varrho$ was still positive but small ($+0.7\times 10^{-3}$). A magnetoresistance effect of the Lorentz type but with the spontaneous Hall field as magnetic field, manifests itself in first approximation as a negative

orientation effect, as is seen from fig. 9. We therefore suggest that this effect is superimposed on the normal orientation effect and accounts for the minus signs in the Mo and Cr alloys as reported by van Elst and Gorter. We see that this is possible as regards the order of magnitude. A consequence would be, that at low temperatures the resistivity, especially that in the transverse direction, increases with the field, just as in fig. 9. Van Elst has informed the author that this is actually the case for these types of alloys.

16. Dependence of ρ on the magnitude of H

We now proceed with the effects of purely ferromagnetic origin.

Fig. 12 shows $-(1/\varrho)(\mathrm{d}\varrho/\mathrm{d}H)$ at room temperature for the alloys Ni-Fe, Ni-Co and Ni-Cu. The value for iron is 4×10^{-8} 1/oersted. The results for Ni-Fe agree with those obtained by Bozorth [33]). In the neighbourhood of Ni_3Fe a superlattice occurs, whilst the rise of the Cu-curve is without doubt due to the lowering of the Curie point.

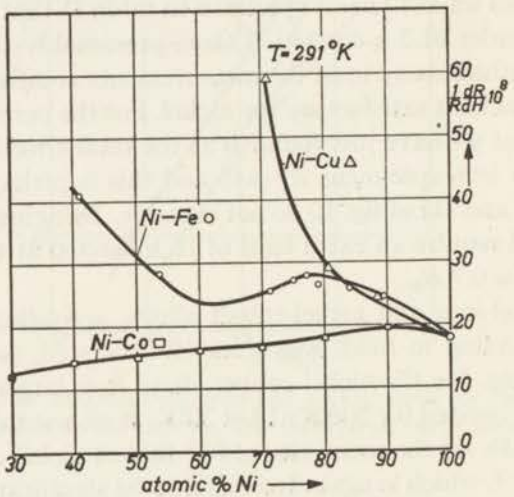

Fig. 12. Relative slopes of the ϱ-H curves in strong fields at room temperature. The value for pure iron is -4×10^{-8} 1/ oersted.

It may be assumed that ϱ depends only on the magnetization, or

$$\mathrm{d}\varrho/\mathrm{d}H = (\mathrm{d}\varrho/\mathrm{d}M)\,(\mathrm{d}M/\mathrm{d}H). \qquad (6)$$

A further assumption is that $\mathrm{d}\varrho/\mathrm{d}M$ does not vary appreciably with M for normal fields, so the dependence of $\mathrm{d}\varrho/\mathrm{d}H$ on H is determined by that of $\mathrm{d}M/\mathrm{d}H$, the intrinsic susceptibility. There are two theories concerning this susceptibility. Akulov's theory [34]), based on the phenomenological Weiss theory, predicts a field-independent $\mathrm{d}M/\mathrm{d}H$, whereas Holstein

and Primakoff[35]) using the Bloch spin waves, including dipole-dipole interaction, derive for strong fields $dM/dH \sim H^{-\frac{1}{2}}$. In the first case the ϱ-H curve should be a straight line, and in the latter a parabola. Of course all these considerations hold only when the Weiss domain structure has disappeared and all magnetization vectors are in the direction of $\mathbf{H}$ ($H > 5000$ oersted). It is rather difficult to decide experimentally between the two possibilities. In one case (Ni89Fe11) we succeeded in determining the field dependence of ϱ with a sufficient accuracy (10^{-5}). The result has been plotted in fig. 13. The four points are situated exactly on a straight line, which is drawn together with the closest fitting parabola. This result points more to the validity of the Weiss theory than to that of the Bloch spin wave theory. Of course the latter holds only at low temperatures, where only relatively few spins are reversed.

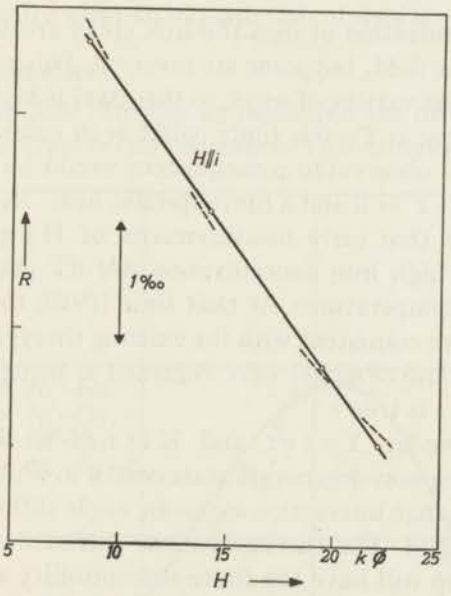

Fig. 13. Resistivity-field curve in a longitudinal field for Ni 89 Fe 11, showing that a linear relationship exists. The dashed curve is the closest fitting parabola $\varrho = a - bH^{1/2}$.

At low temperatures the slope must vanish because saturation is reached and dM/dH consequently is zero. This was verified for alloys containing besides nickel 10—30% iron, 10—70% cobalt and 10—20% copper. At $T = 77°K$, $-(1/\varrho)\,(d\varrho/dH)$, never exceeded 8×10^{-8} 1/oersted. The alloy Ni40 Fe60 behaves in quite an anomalous way: $-(1/\varrho) \times (d\varrho/dH)$ at low temperatures (44×10^{-8} 1/oersted) was found to be even greater than at room temperature (41×10^{-8} 1/oersted). This might be explained by assuming that even at $T = 0°K$ no complete alignment of spins exists, and consequently

$dM/dH \neq 0$. These singularities may be accounted for by the negative exchange interaction between the spins of the iron atoms in the γ-phase, since γ iron is non-magnetic.

The theory for different types of exchange interactions has been developped by Néel [36] for the ferrites. The exchange energy is then of the form

$$E_{exch} = -\tfrac{1}{2}\alpha M_{Ni}^2 - \beta M_{Ni} M_{Fe} - \tfrac{1}{2}\gamma M_{Fe}^2. \qquad (7)$$

If the three exchange parameters α, β and γ are positive, the energy is as low as possible for the maximum values of the magnetic moments. In our case γ is negative, and then there is a critical value of M_{Fe}, and thus of the concentration of the iron atoms, above which E is no longer extreme for the saturation value of M_{Fe}. This value is

$$M_{Fe} = -(\beta/\gamma)\, M_{Ni}. \qquad (8)$$

For a greater concentration of iron the iron spins are according to Néel not all parallel to the field, but some are reversed. This reversing of the spins can be done in a great variety of ways, so this state is highly degenerate, and therefore the entropy at $T=0$ is finite, what is in conflict with Nernst's theorem. One of its observable consequences would be a finite slope [37] of the $M - T$ curve at $T = 0$ and a finite specific heat. In this connection it is interesting to note that early measurements of Hegg [38] indicate that for Ni alloys with high iron concentration dM/dT does not vanish down to liquid nitrogen temperatures. At that time (1910) these curves were the only ones which were consistent with the existing theory. The $M - T$ curves of the other alloys and of nickel were regarded as being anomalous. At present just the reverse is true.

It has been shown by Yafet and Kittel [39] that in such cases in ferrites a lower lying non-degenerate state exists, in which the spins with the counteracting exchange interaction make an angle different from 0° or 180° with the applied field. The thermodynamic difficulties are then no longer present, whereas we still have the finite susceptibility at $T = 0$.

Also the application of the band model to the 3*d* electrons removes the degeneracy. Then the various states have different kinetic energy. Also in this case there is the finite susceptibility at $T = 0$.

The concentration, corresponding to that of (8), of the nickel ions below which the orientation of the iron spins ceases to be complete, even at the absolute zero, can be derived from the experiments. For the Ni53Fe47 alloy the slope had not yet disappeared completely $-(1/\varrho)\,(d\varrho/dH) = 13 \times 10^{-8}$ 1/oersted at 77°K and 7×10^{-8} at 20°K), so we may assume that this critical composition is about Ni60Fe40. For the Ni70Cu30 alloy there was also still a small slope at $T = 20$°K (11×10^{-8} 1/oersted), but this must have a different cause.

So far, all peculiar features of $d\varrho/dH$ were explained in terms of those of

dM/dH, and the cause of $d\varrho/dM$ was left undiscussed. We shall see in section 18 that the resistivity in the ferromagnetic state is a factor 2 or 3 smaller than in the paramagnetic state, if it should exist at the same temperature, as follows from extrapolation of the ϱ-T curve from temperatures above the Curie point towards lower temperatures. We conclude that $d\varrho/dM < 0$, and assume that it is of the order of $(\varrho_{ferro} - \varrho_{para})/M$. This means that then $d \ln \varrho / d \ln M$ is of the order of unity. We put

$$(1/\varrho)\, d\varrho/dH = (d \ln \varrho / d \ln M)\, (1/M)\, dM/dH.$$

The experimental values of $(1/\varrho) d\varrho/d H$ are about 2×10^{-7} 1/oe. For nickel Polley [40] found at roomtemperature $dM/dH = 1.3 \times 10^{-4}$, so that $(1/M)\, dM/dH$ is 2.6×10^{-7}, which value is in fair agreement with that of $(1/\varrho)\, d\varrho/dH$, so that our assumption regarding $d \ln \varrho / d \ln M$ seems to be valid. The explanation of the difference in the para and ferromagnetic state will then automatically yield an explanation of $d\varrho/dH$.

17. The orientation effect

For the polycrystalline samples we measured the difference between the longitudinal and the transversal resistance. This difference was always posi-

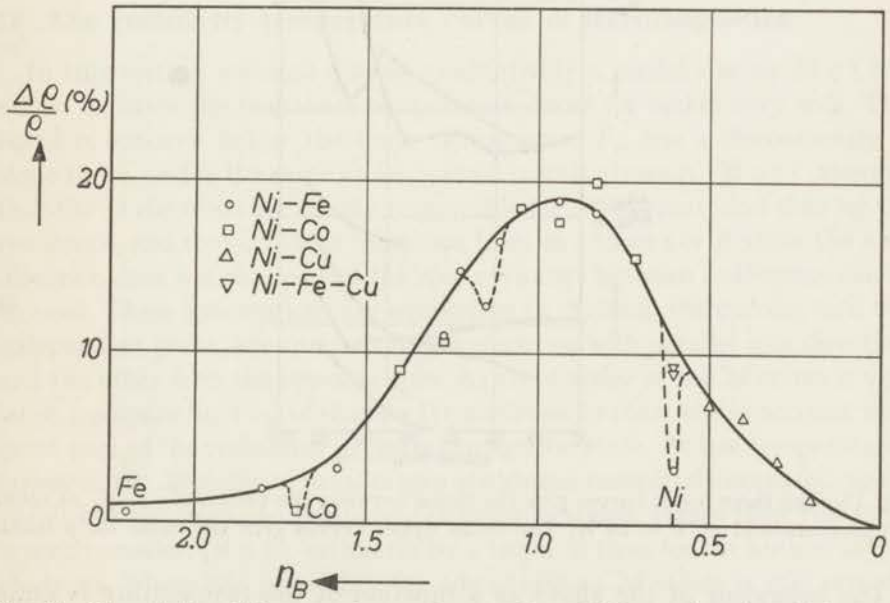

Fig. 14. The relative difference of $\varrho_{/\!/}$ and $\varrho_{\perp}$ at $T = 20°K$ as a function of the mean number of Bohr magnetons. Note the small values of the pure metals Ni and Co and of the ordered alloy Ni_3Fe. The values for Ni60Cu40 and the Ni-Fe-Cu alloys ($n_B = 0.6$) are taken from van Elst and Gorter [32]).

tive, in contradistinction to the magnetostriction. In fig. 14 the relative change in resistance, $(\varrho_{/\!/} - \varrho_{\perp})/\varrho$ extrapolated to $H = 0$, at $T = 20°K$, has

been plotted as a function of the mean number of Bohr magnetons n_B. For ϱ has been taken $\varrho = \frac{1}{3}\varrho_{/\!/} + \frac{2}{3}\varrho_{\perp}$.

It occurred already to S n o e k [41]) that this anisotropy of the resistivity has a maximum at about $n_B = 1$. At the same point the linear magnetostriction goes through zero. Actually these observations were the starting point for these investigations. We have seen in chapter II that at about this value of n_B also the spontaneous Hall effect vanishes. The connection between these three facts is not yet clear.

We see that the values for all alloys are nearly a function of the Bohr magneton number only. Exceptions occur for the alloys Ni_3Fe and for the pure metals Ni and Co. For Co the value given by B a t e s [42]) has been taken, assuming that $\Delta\varrho/\varrho$ does not vary appreciably with temperature. This was verified in the case of Ni, where the effect at 77°K was only 12% greater than at room temperature.

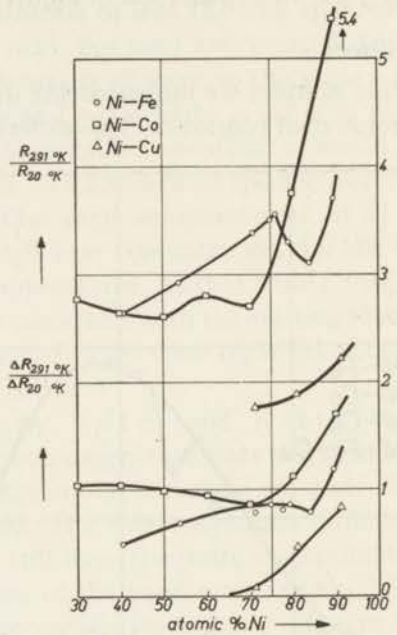

Fig. 15. The three lower curves give the ratios between the values of $\varrho_{/\!/} - \varrho_{\perp}$ at room temperature and at $T = 20$°K. The three upper curves give the same for ϱ itself.

The behaviour of the alloys as a function of the temperature is quite different from that of the pure metals. There $\Delta\varrho$ itself does not vary appreciably with temperature. In fig. 15 the ratios between $\Delta\varrho$ at room temperature and at low temperature and also those of ϱ are given. The curves approach the values for pure nickel, which are 144 and 163 respectively. Measurements with non-annealed samples showed always smaller values for $\Delta\varrho/\varrho$.

Some measurements have been made on samples (Ni-Fe 79—21 and

89—11) having a marked texture, so it may be expected that they behave as single-crystals. We were able to measure ϱ_3 of equation (1) at different temperatures (see fig. 16). The most interesting result is the strong decrease of $\varrho_3/\varrho_{T=0}$ with increasing temperature.

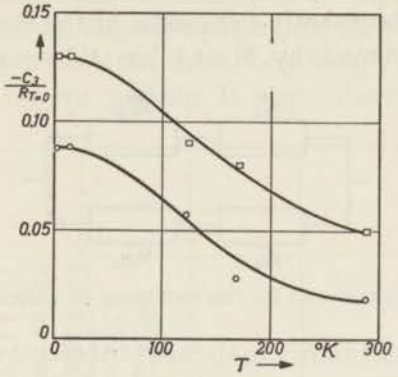

Fig. 16. The anisotropy of the orientation effect as a function of temperature.
□ = Ni 89 Fe 11
○ = Ni 79 Fe 21

18. The resistivity-temperature curves of ferromagnetics

In this section we shall discuss qualitatively a model due to M o t t [43]) which explains the resistance-temperature curve for nickel very well. This curve is concave below the Curie temperature T_c, has a discontinuity in slope there, and is the same as for normal metals above it. M o t t assumes that the 4*s* electrons are mainly responsible for the current, and thus for the resistance, and that during a transition from an *s* to an *s* or d state the spin direction does not change and the spin exchange between *s* electrons can be ignored. These assumptions are equivalent to dividing the current into two independent parts, one current of the *s* electrons with parallel spin direction, and the other with the opposite spin. As the density of the 3*d* states is very large, (compare fig. 1—3 of chapter I) transitions to these states account for a great part of the resistance in the paramagnetic state. At low temperatures, however, the 3*d* states of parallel spin are almost completely occupied, so the parallel 4*s* electrons can jump only to other 4*s* states. Hence their resistance is much smaller (M o t t estimates by a factor 5) than for the antiparallel 4*s* electrons, where the possibility for transitions to 3*d* states is still present. Therefore at low temperatures we may assume that the resistance is determined mainly by the *s*—*s* transitions of the electrons with parallel spin. This state of affairs may be demonstrated by the scheme of fig. 17. In the paramagnetic state the two branches of the circuit are equal ($R_{sds} \approx 4R_{ss}$, R_{ss} is due to direct *s*—*s* transitions, and R_{sds} via a *d* state). At low temperatures R^{+}_{sds} drops out. The influence of the magnetic field strength as dis-

cussed in section 16 can be explained as a decrease of the density at the Fermi surface of the parallel $3d$ states with increasing magnetization, resulting in a decrease of the resistance (R^{+}_{sds}).

We have seen in chapter I that there is a considerable mixing of the $4s$ and $3d$ states, but that there is still a band in which an appreciable part of the electrons has predominantly s character at the Fermi surface, so that a distinction as has been made by Mott has still sense.

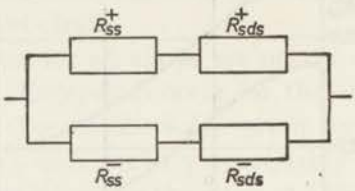

Fig. 17. Schematical circuit for the resistance of a ferromagnetic metal.

We will also apply this theory to the alloys of nickel with magnetic or non-magnetic ions. At low temperatures these foreign atoms represent the only scattering centres. The perturbing potentials are practically confined to these regions. For the nickel alloys with cobalt or iron the $3d$ bands are modified at the positions of the foreign atoms, but still at these places there are unoccupied $3d$ orbits, and the perturbing potentials, which are just finite at these ions, can cause s—d transitions, so that Mott's picture remains valid also for these alloys. This is presumably not the case for the nickel alloys with non-magnetic inclusions, since at the places where the perturbing potential is large, no empty $3d$ orbits are present with comparable energy.

In order to verify this experimentally, we have measured the resistivity for varying temperature of some alloys. If we plot the results $\{\varrho(T) - \varrho(0)\}/\{\varrho(T_c) - \varrho(0)\}$ as a function of the reduced temperature T/T_c, (fig. 18), where T_c is the Curie temperature, we can compare all alloys with the curve for nickel. We see then that indeed the alloys with non-magnetic additions such as V or W have the smallest discontinuity of slope at the Curie temperature, and are less concave than the Ni-curve. The Sn alloy behaves like the alloys with ferromagnetic constituents. The change in slope at T_c does not vanish of course, since at finite temperatures Mott's picture is again valid to some extent. The values of ϱ are given in table III.

TABLE III

Resistivities and Curie temperatures of Fe and some Ni-alloys			
Comp. at. %	T_c(°K)	ϱ(0°K) $\times 10^6$ (Ω cm)	$\varrho(T_c) \times 10^6$ (Ω cm)
Fe 100	1047	0.0	103.0
Ni 100	623	0.0	28
Ni 80 Co 20	851	3.9	62.0
Ni 90.7 Cu 9.3	523	9.0	38.4
Ni 98.5 Sn 1.5	577	4.7	34.7
Ni 96.6 W 3.4	457	21.6	40.8
Ni 96.6 V 3.4	500	19.0	42.5

We have also measured the resistivity *versus* temperature curve of pure iron which is very similar to that of nickel. Iron has a Bohr magneton number of 2.2. These non-integral values, which also occur in nickel and cobalt (0.6 and 1.7 respectively), are easily explained by the band model for the *d* and *s* electrons, which has been discussed in chapter I, and one assumes then, neglecting the orbital angular momentum, that there are 0.6 and 0.7 electrons in the *s* band in the latter cases. Accordingly iron should have only 0.2 *s* electrons, what is very unlikely. It seems therefore plausible, as has

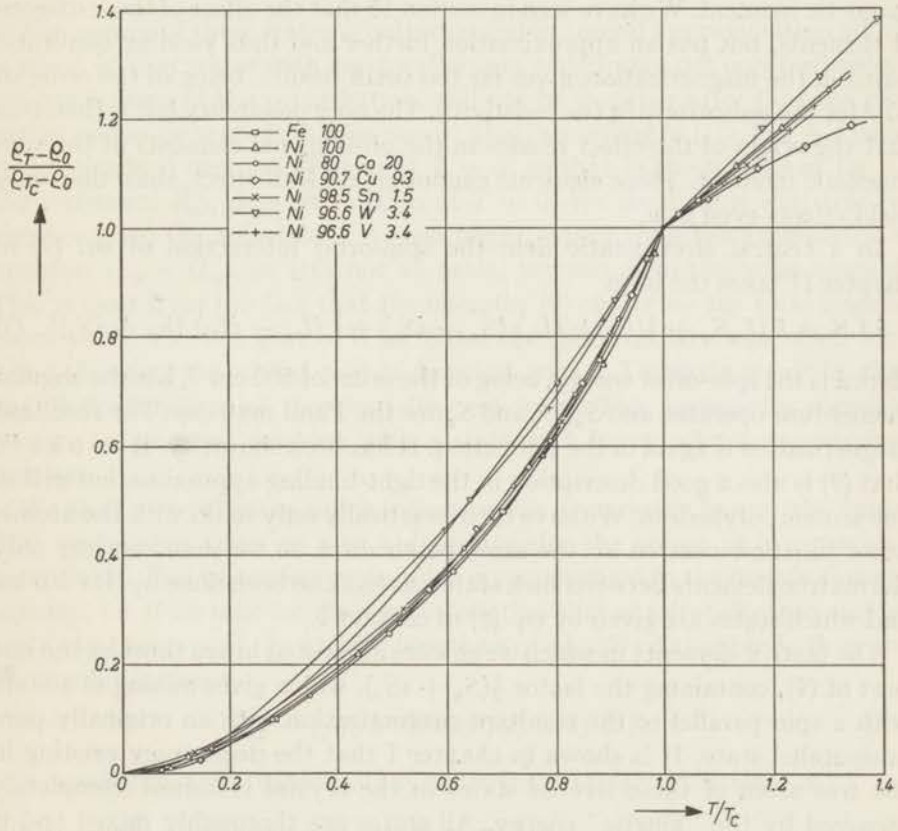

Fig. 18. Reduced resistivity-temperature curves of some ferromagnetic alloys and of iron and nickel. The curve for nickel has been taken from literature.

been pointed out by Stoner[44]) that the half band of parallel *d* spins is not completely occupied due to the large kinetic energy which would be involved. But then *s*—*d* transitions with parallel spin are possible at all temperatures, so this resistivity theory of Mott is in this case not consistent with the theory of Stoner for the saturation magnetization. According to Stoner's picture the paramagnetic susceptibility should be finite at $T = 0$. The measurement of the ϱ—H curve of a silicon-iron alloy at low temperatures might provide a solution of this problem.

19. Theory of the orientation effect

So far no cause for an anisotropy in the resistance is present, at a given orientation of the magnetization. In our opinion this can only be introduced by the interaction between the spin system and the lattice *via* the spin-orbit coupling.

In chapter II we were interested in effects odd in the magnetization, and used therefore only the diagonal elements of the spin moment operator. For the anisotropy in the resistivity we have to look for effects which are even in the magnetic moment. We have seen in section 15 that the effect of these diagonal elements, but put an approximation further and thus yielding quadratic terms in the magnetization, gives far too small results, being of the order of 10^{-3} for the anisotropy in the resistivity. The only possibility left is therefore that the origin of the effect resides in the off-diagonal elements of the spin magnetic moment. These elements cannot give a Hall effect, since they only yield effects even in μ_z.

In a central electrostatic field the spin-orbit interaction of eq. (9) of chapter II takes the form

$$\lambda \mathbf{LS} = \lambda \{L_z S_z + \tfrac{1}{2}(L_x + iL_y)(S_x - iS_y) + \tfrac{1}{2}(L_x - iL_y)(S_x + iS_y)\} \quad (9)$$

Here λ is the spin-orbit energy, being of the order of 500 cm^{-1}, $\mathbf{L}$ is the angular momentum operator and S_x, S_y and S_z are the Pauli matrices. The resultant magnetization is again in the z direction. It has been shown by Brooks [45] that (9) is also a good description in the tight-binding approximation within one atomic polyhedron. We have then practically only to do with the atomic wave function centred at the same polyhedron, so we shall consider only the matrix elements between such states, as has also been done by Brooks and which states are given by eq. (5) of chapter I.

The matrix elements in which we now are interested in are those of the last part of (9), containing the factor $\frac{1}{2}(S_x + iS_y)$, which gives mixing of a state with a spin parallel to the resultant magnetization with an originally pure antiparallel state. It is shown in chapter I that the degeneracy existing in the free atom of these five $3d$ states in the crystal is almost completely removed by the "kinetic" energy. All states are thoroughly mixed and it cannot be said with certainty which atomic wave function predominates at the Fermi level. We shall therefore make the crude approximation that all states equally occur there and that the differences in energy between combining states all have the same value ε. This energy difference is composed of electrostatic, kinetic, and exchange energy. It is then possible to use the eigenfunctions of the L_z operator which have angular dependent coefficients

$$\varphi_2 \sim (x + iy)^2, \quad \varphi_1 \sim 2z(x + iy), \quad \varphi_0 \sim (\tfrac{2}{3})^{\frac{1}{2}}(2z^2 - x^2 - y^2)$$
$$\varphi_{-1} \sim 2z(x - iy), \quad \varphi_{-2} \sim (x - iy)^2.$$

If we denote the spin functions by the superscripts + and −, we find that the last term of (9) in first approximation changes the wave functions of the electrons with antiparallel spin orientation into:

$$\begin{aligned}
\psi_2^- &= \varphi_2^- - 2\,(\lambda/\varepsilon)\,\varphi_1^+ \\
\psi_1^- &= \varphi_1^- - 6^{\frac{1}{2}}\,(\lambda/\varepsilon)\,\varphi_0^+ \\
\psi_0^- &= \varphi_0^- + 6^{\frac{1}{2}}\,(\lambda/\varepsilon)\,\varphi_{-1}^+ \\
\psi_{-1}^- &= \varphi_{-1}^- + 2\,(\lambda/\varepsilon)\,\varphi_{-2}^+ \\
\psi_{-2}^- &= \varphi_{-2}^-
\end{aligned} \tag{10}$$

The energy of these states is only changed in second approximation which is small, so that states with antiparallel spin which were not occupied before the application of the perturbation, will not be so either after that the perturbation has been applied. This means, that, according to (10), the + d band is not occupied completely even at $T = 0$, so that in the scheme of fig. 17 the resistance R_{sds}^+ does not vanish at $T = 0$. We shall show that this resistance gives the anisotropy. As one might expect from the asymmetry of operator $(L_x - iL_y)$, in (10) not all orbits are mixed to the same amount. This is clear from the fact that the operator (9) conserves the total angular momentum. The last part of it increases the spin angular momentum with $\hbar$ and therefore the orbital part is dereased with $\hbar$. The main result is, that in (10) the function φ_2^+ therefore does not occur. This asymmetry comes in because φ_{-2}^- cannot combine with a state with lower orbital angular momentum.

We shall now calculate which influence this asymmetry has on the transition probability from an s to a d state under the action of a perturbing potential V. This transition probability is proportional to the matrix element squared, *i.e.* if we take for the s wave function that of a free electron and for the d electron one of the atomic functions of eq. (5) of chapter I, then one obtains for instance

$$P_{sd} \sim |\iiint e^{-i\mathbf{kr}} V xy\, f(r)\, \mathrm{d}x\mathrm{d}y\mathrm{d}z\,|^2. \tag{11}$$

Assuming that V is spherically symmetrical, (11) is proportional to

$$P_{sd} \sim k_x^2\, k_y^2\, g\,(k). \tag{12}$$

The wave functions in (11) are not orthogonal, but the ignored terms are proportional to the overlap integral and do not change the orientation properties of (12). As it may be expected that in the mean V does not possess extremely large orientation properties, (12) is the most anisotropic function which can be obtained. We see that in this case electrons moving in the z-direction, thus parallel to the magnetization, cannot be trapped.

Comparing (12) with (11) we see that for a spherically symmetrical perturbing potential the transition probability has the same angular dependence in **k** space as the charge distribution in normal space. Applying this result

to (10), we find for the average probability for an $s-d$ transition in the resistance R^{+}_{sds}

$$P_{sd} \sim (k^2 + k_z^2)\, g\,(k). \tag{13}$$

Electrons moving in the z direction (parallel to the magnetization) are therefore most easily trapped, so we can now already conclude that $\varrho_{/\!/} > \varrho_{\perp}$, in agreement with the experiments.

The evaluation of the anisotropy in the resistance is now straightforward. Assume that in the unperturbed state (only R^{+}_{ss} present) there is an isotropic time of relaxation τ_0. This will be slightly changed by an anisotropic term

$$\tau(\mathbf{k}) = \tau_0(E) - \tau_1(\mathbf{k}), \quad \tau_1 \ll \tau_0.$$

This holds for the parallel electrons. Assuming, as already done tacitly, that the energy is conserved during a transition, $\tau(\mathbf{k})$ has to satisfy

$$\int P\,(\mathbf{k}\,\mathbf{k}') \left\{\tau(\mathbf{k}) - \frac{k_i'}{k_i}\,\tau(\mathbf{k}')\right\} \mathrm{d}S' = \text{constant},$$

where the integration has to be taken over the spherical Fermi surface in $\mathbf{k}'$-space. The index i refers to the direction of the current. From (13) it follows that $P(\mathbf{k}\mathbf{k}')$ is of the form

$$P(\mathbf{k}\mathbf{k}') = P_0 + P_1 \quad P_1 \ll P_0,$$

with

$$P_1 \sim (k^2 + k_z^2)\ (k^2 + k_z'^2),$$

where P_0 is due to direct $s-s$ scattering, and P_1 via d states for the electrons with parallel spin orientation.

Assuming that P_0 is isotropic, to a first approximation one finds

$$\tau_1 \sim k^2 + k_z^2,$$

and

$$\varrho_{/\!/} \sim 1 + 4\Delta \qquad \varrho_{\perp} \sim 1 + 3\Delta, \tag{14}$$

Δ being a positive constant and approximately equal to the relative difference between the longitudinal and the transverse resistivity. According to (10) and (14), $(10/3)\Delta$ corresponds to an admixture of $4\,(\lambda/\varepsilon)^2\,\varphi^{+}$ state per ψ^{-} state, so we find

$$(\varrho_{/\!/} - \varrho_{\perp})/\varrho \sim \Delta \sim (3/10) \times 4\,(\lambda/\varepsilon)^2\ R_{sds}/R_{ss}.$$

In order to estimate the order of magnitude, we make use of the fact that in the theory of the spectroscopic splitting factor g also a ratio of λ and a similar energy difference ε' occurs. According to Fletcher[7] $(g - 2)$ is of the order of $8\lambda/3\varepsilon'$, so that we shall take $(\lambda/\varepsilon)^2 \approx 0.01$. Assuming with Mott[43] $R_{sds}/R_{ss} \approx 4$, we finally find

$$(\varrho_{/\!/} - \varrho_{\perp})/\varrho \approx 0.05, \tag{15}$$

being of the right order of magnitude, though somewhat too small to account for the highest values.

20. Discussion

The theoretical results of section 19 were obtained by assuming that the perturbing potential V is spherically symmetrical. This applies to the perturbing potential caused by foreign atoms in solid solution in disordered alloys. We have seen in section (18) that, for causing $s-d$ transitions, these foreign atoms have to be ferromagnetic. Our theory applies therefore to alloys of nickel with cobalt or iron. The fact that points for copper also lie on the same curve of fig. 14 suggests that in the latter alloys the same mechanism is working, *i.e.* also the copper ions have opened their d shells as in many salts and are here ferromagnetic.

The fact that the values of the Ni-Co and the Ni-Fe alloys are lying on one curve, suggests that the band picture for the $3d$ electrons is valid here. The curve is then in some way related to the density of states curve. Calculations show [3] [46]) that the latter curve has a maximum for n_B comparable with unity, and then falls off rapidly. This is in agreement with our $\Delta\varrho/\varrho$-curve.

Lattice vibrations and internal stresses will give perturbing potentials which only in the mean, *i.e.* averaged over the crystal, are spherically symmetrical, but the V occurring in (11) is anisotropic. As a consequence the resultant anisotropy in the transition probability will be less, and we may expect that the thermal resistivity and that due to internal stresses will give a smaller anisotropy. This can be demonstrated easily for the case of lattice vibrations. The perturbing potential due to a lattice wave with wave vector $\mathbf{q}$ is proportional to $e^{i\mathbf{qr}}$. We see then that in (11) $\mathbf{k}$ is replaced by $\mathbf{k} + \mathbf{q}$, so that for instance also an electron moving in the z direction can now be captured in an xy orbit. Since $\mathbf{q}$ can have all orientations, the anisotropy in $P(\mathbf{kk}')$ will be smaller. This is in agreement with the experimental values for the non-annealed samples and for the pure metals Ni and Co, which lie below the curve. The substantially higher values of the two "pseudo nickels" ($\Delta\varrho/\varrho \sim$ $\sim 9.5\%$) confirm our theory.

At finite temperatures the anisotropy due to the foreign atoms and that caused by the thermal lattice vibrations are present at the same time. In any case it is clear that, because of the small effect of the lattice vibrations, $\Delta\varrho$ will only increase slightly with increasing temperature, or even decrease, due to the decrease in saturation magnetization, which is in agreement with the experiments (see fig. 15). For nickel $\Delta\varrho/\varrho$ is practically constant, its small decrease can be explained again by the decrease in M with increasing T.

The measurements of van Elst and Gorter [32]) show that for most alloys with non-magnetic constituents $\Delta\varrho/\varrho$ at low temperatures is smaller than 1%, confirming our predictions. (These are the V, Cr, Mo and Walloys.) The negative values of the Cr and the Mo alloy have been explained

above, so that it is reasonable to assume that the real anisotropy in the resistivity is always positive ($\varrho_{/\!/} > \varrho_{\perp}$). In some cases, however, (the Al, Si and the Sn alloys) $\Delta\varrho/\varrho$ is of the order of 3%. It is well known that Sn does not form solid solutions with Ni, as was also remarked by van Elst and Gorter. Furthermore the solid solubility of Al in Ni is 4% and of Si about 6% (weight %). The other alloys cited above with a small value of $\Delta\varrho/\varrho$ all have a very large solid solubility (V: 20%, Cr: 45%, Mo: 17%, W: 30%).

Precipitations will cause large internal strains in the matrix. These strains form perturbing potentials for the electrons, but now these potentials are at the places of the Ni ions which can then trap conduction electrons in the holes of their d shells. This is favourable for the existence of anisotropy in the resistivity and for a concave ϱ — T curve (compare the curve for the Sn alloy in fig. 18). This anisotropy can then be of the order of 3%, just as in Ni for the lattice vibrations. We assume therefore that also in the Al and Si alloys we have not a perfect solid solubility. This is in agreement with the fact that the 4.5% Al alloy is very hard, due to internal stresses, and is known as Z-nickel [47]). For the Si alloy it is a little doubtful, but in any case we may expect that in this 5% alloy, which is very near to the limit of 6% of solid solubility, large internal stresses will occur. The value of $\Delta\varrho/\varrho$ is therefore intermediate. A direct test of this hypothesis can be obtained by measuring the value of $\Delta\varrho/\varrho$ at low temperatures of alloys with a low content of Al and Si, *e.g.* 2%, which goes into solid solution. One should expect that the values of $\Delta\varrho/\varrho$ are then comparable with those of the other solid solutions, *e.g.* smaller than 1%. We should have then the peculiar fact that $\Delta\varrho/\varrho$ as a function of the composition goes through a minimum.

A more indirect confirmation of the suggestion is formed by the fact that for the alloys with $\Delta\varrho/\varrho < 1\%$ the value of $\Delta\varrho/\varrho$ increases with temperature as was already noticed by van Elst and Gorter. For instance, for the Cr alloy it is −0.16% at 14°K and +0.11% at 77°K, showing that the part of ϱ dependent upon temperature contributes about 2% to $\Delta\varrho$. This is presumably due to the fact that the lattice vibrations give perturbing potentials at the places of the nickel ions. One should also expect that for these alloys $\Delta\varrho/\varrho$ increases by plastic deformation, the reverse being the case for the alloys with magnetic constituents.

The Mn ions in the Mn alloy are ferromagnetic for low concentrations, each contributing about 2.8 μ_B. Therefore $\Delta\varrho/\varrho$ is of the same order of magnitude as for the Ni-Fe or Ni-Co alloys.

REFERENCES

1) J. H. van Vleck, Rev. mod. Phys. **25**, 220 (1953).
2) G. C. Fletcher and E. P. Wohlfahrt, Phil. Mag. **42**, 106 (1951).
3) G. C. Fletcher, Proc. phys. Soc. **A 65**, 192 (1952).
4) P. O. Lödwin, J. chem. Phys. **18**, 365 (1950).
5) D. R. Hartree and W. Hartree, Proc. roy. Soc. **A 157**, 490 (1936).
6) E. P. Wigner and F. Seitz, Phys. Rev. **43**, 804 (1933).
7) G. C. Fletcher, Proc. phys. Soc. **A 67**, 505 (1954).
8) E. M. Pugh and N. Rostoker, Rev. mod. Phys. **25**, 151 (1953).
9) W. L. Webster, Proc. Cambr. phil. Soc. **23**, 800 (1925).
10) N. Rostoker and E. M. Pugh, Phys. Rev. **82**, 125 (1951).
11) C. J. Kevane, S. Legvold and F. H. Spedding, Phys. Rev. **91**, 1372 (1953).
12) J. P. Jan and H. M. Gijsman, Comm. 288*a* K.O. Lab., Physica, Den Haag **18**, 339 (1952).
13) A. W. Smith, Phys. Rev. **30**, 1 (1910).
14) A. N. Gerritsen and W. J. de Haas, Comm. 261*b* K.O. Lab., Physica, Den Haag **7**, 802 (1940).
15) J. Volger, Phys. Rev. **79**, 1023 (1950).
V. Frank, Appl. sci. Res. **B 3**, 129 (1953).
16) S. Foner and E. M. Pugh, Phys. Rev. **91**, 20 (1953).
17) E. M. Pugh, Phys. Rev. **97**, 647 (1955).
18) J. P. Jan, Helv. phys. Acta **25**, 677 (1952).
19) C. Kooy, Phys. Rev. **95**, 843 (1954).
20) L. I. Schiff, Quantum Mechanics, Mac Graw Hill Book Co. Inc., New York (1949) Chapter XII.
21) G. H. Wannier, Phys. Rev. **72**, 304 (1947).
22) A. G. Samolovich and B. L. Konkov, J. exp. theor. Phys. (U.S.S.R.) **20**, 783 (1950).
23) V. Rudnitsky, J. exp. theor. Phys. (U.S.S.R.) **9**, 262 (1939).
24) R. Karplus and J. M. Luttinger, Phys. Rev. **95**, 1154 (1954).
25) L. I. Schiff, Quantum Mechanics, Mac Graw Hill Book Co. Inc., New York (1949), p. 77.
26) N. F. Mott and H. S. W. Massey, The Theory of atomic Collisions, Oxford (1949), p. 24.
27) C. Kittel, Phys. Rev. **76**, 743 (1949).
28) S. Foner, Phys. Rev. **88**, 955 (1952).
29) Cf. R. M. Bozorth, Ferromagnetism, D. van Nostrand Inc., New York (1951) Chapter 16.
30) Ref. 29, p. 765.
31) M. Kohler, Ann. Physik (5) **32**, 211 (1938).
32) H. C. van Elst and C. J. Gorter, Comm. 295*b* K.O. Lab., Appl. sci. Res. **B 4**, 87 (1954).
33) R. M. Bozorth, Phys. Rev. **70**, 923 (1946).
34) N. S. Akulov, Z. Phys. **69**, 822 (1931).
35) T. Holstein and H. Primakoff, Phys. Rev. **58**, 1098 (1940).
36) L. Néel, Ann. Physique **3**, 137 (1948), **5**, 232 (1936).
37) H. B. G. Casimir and C. J. Gorter, Disc. Remarks, J. Phys. Rad. **12**, 251 (1951).
38) F. Hegg, Arch. sci. Phys. nat. **30**, 15 (1910).
39) Y. Yafet and C. Kittel, Phys. Rev. **87**, 290 (1952).
40) H. Polley, Ann. Physik **36**, 625 (1939).
41) J. L. Snoek, Nature **163**, 837 (1949).
42) L. F. Bates, Proc. phys. Soc. **A 58**, 153 (1946).
43) N. F. Mott, Proc. roy. Soc. **A 153**, 699 (1936).
44) E. C. Stoner, Rep. Progr. Physics **10**, 43 (1948).
45) H. Brooks, Phys. Rev. **58**, 909 (1940).
46) G. F. Koster, Phys. Rev. **98**, 901 (1955).
47) R. M. Bozorth, Ferromagnetism, D. van Nostrand Inc., New York (1951),p. 299.